I. Final Report for DOE SBIR Phase I Project DE-SC0013795

Microtron-based Compact, Portable Gamma-Ray Source

Final Report for Phase I SBIR Project start date: June 8, 2015, end date: April 7, 2016

Principal Investigator: Dr. Robert J. Abrams

Muons, Inc., 552 N. Batavia Ave., Batavia, IL 60510

Approved for public release; further dissemination unlimited. (Unclassified Unlimited)

PREPARED FOR THE UNITED STATES DEPARTMENT OF ENERGY

Work Performed under SBIR grant DE-SC0013795

Phase I Final Technical Report

Microtron-based Compact, Portable Gamma-Ray Source

Table of Contents

II. Proprietary Data Legend – Not Applicable.

III. Project Overview

The objective of Phase I of this project was to produce a conceptual design of a prototype compact microtron electron accelerator, which could be designed, built, and demonstrated in Phase II of the project. The conceptual design study included an analysis of the parameters of the microtron and its components, and the expected performance of the prototype microtron as a source of x-rays and/or RF neutrons in the MeV energy range. The major components of the microtron are the magnet, the accelerating system, the power system, the vacuum system, the control system, the beam extraction system and the targets to produce x-rays (and/or neutrons). Our objectives for the design of the prototype were for it to be compact, cost-effective, capable of producing high intensity x-ray (an/or neutron) fluxes. In addition, the prototype was to be easily assembled and disassembled so that components could be easily replaced.

The main parameters for the prototype are the following: the range of electron kinetic energies, the output power, the RF frequency band (X-band, C-band, or S-Band), the type of injection (Type I or Type II), the magnet type, i.e. permanent magnet, electromagnet, or a hybrid combination of permanent and electromagnet.

The results of the Phase I study and analysis for a prototype microtron are the following: The electron energy range can be varied from below 6 MeV to 9 MeV, the optimal frequency range is S-Band (2-4 GHz) RF frequency, Type II injection (described below), and the magnet type is the hybrid version. The prototype version will be capable of producing gamma ray doses of ~1800 R/min-m and neutron fluxes of up to ~6 x 10^{10} n/s with appropriate targets. The results of the Phase I study and analysis are provided below.

The proposed Phase II plan was to demonstrate the prototype at low beam power. In the subsequent Phase III, high power tests would be performed, and the design of commercial versions of microtrons with various energies, sizes and types would be produced and marketed, including a more compact and more portable 6 MeV battery-powered model that more closely meets the requirements in the original FOA topic description.

In the course of the Phase I study, we also identified another microtron version, one that was larger (not compact) and more powerful than that of the Phase II prototype, which could serve as an intense source of photo- neutrons, up to 4 x 10^{12} n/s for use in nuclear medicine, short-lived isotope production, or other applications. In addition, it could produce gamma dose rates up to 130 kR/min-m with a heavy metal bremsstrahlung target. The results and specifications of this were submitted to IPAC16 (Reference [12]) the paper is included in Addendum B. Because this version was beyond the scope of the Phase I project, there is no additional description in the Final Report.

IV. Identification and Significance of the Problem or Opportunity, and Technical Approach

A. Identification and Significance of the Problem or Opportunity

As stated in the FOA, Topic 5d is a subtopic of Topic 5, which is *Neutron and Gamma Sources for Interrogation.*
The complete text of the solicitation for topic 5d is the following:
"Betatron or Equivalent Gamma Source
Develop and demonstrate a portable betatron or equivalent gamma source that provides 1 – 6 MeV gamma rays with a variable duty cycle. The goal is for the system to be less than 100 lbs and run on battery power".

The specific opportunity as defined in Topic 5d is for very compact and portable gamma ray sources that can be deployed in field locations that may be not accessible or practical for larger, more commonly used gamma ray interrogation systems at fixed locations. If the costs of such compact sources are attractive, there are opportunities for use of larger numbers of these systems than for larger and more powerful interrogation systems, perhaps hundreds in the United states, and a similar number abroad. With the stated limit of 6 MeV for gamma rays, the maximum electron accelerator energy required, 6 MeV to 6.5 MeV, is below the energy required for production of neutrons. This is both an advantage and a limitation. The advantage is that the shielding required for gamma rays is less than if neutrons are produced. The limitation is that interrogation by neutrons is not possible, which, if needed, would require a higher energy electron beam, up to about 9.5 MeV. Thus, there is a further opportunity for use of a dual energy accelerator, e.g. with capabilities for up to 6.5 MeV and up to 9.5 MeV electron beams.

Another opportunity has to do with the nature of microtrons as being equivalent to betatrons, as stated in the text of Topic 5d. Microtrons are equivalent to betatrons in that they both are circular electron accelerators, however, microtrons differ in that they use an RF accelerating cavity and a fixed magnetic field instead of a time-varying field, and microtrons are capable of much higher beam intensities, perhaps 100-fold compared to betatrons. This provides opportunities for much faster interrogation scanning times, or to provide greater sensitivity, or both, whichever may be needed more.

As shown in Section B, the conclusion of our Phase I technical evaluation was to propose in Phase II to design, build and test a prototype accelerator that could be operated both at 9.5 MeV and at 6.5 MeV or lower, which could then be the basis for a line of microtron accelerators, ranging a compact, portable gamma source that could operate on batteries and utilize a permanent magnet, to higher energy versions that could be used to produce beams of higher energy gamma rays or intense neutron fluxes
.
These combined capabilities are very attractive for the microtron to be used for interrogation purposes as a neutron source in addition to being a gamma ray source. These capabilities also provide benefits to commercial applications. As described in the following section, our Phase I studies showed that a different parameter set from that in our Phase I proposal would result in a somewhat larger but portable microtron, which has higher dose capabilities, lower cost, greater reliability, with additional capabilities as a intense neutron source and for which a prototype could be successfully built and prepared for test in Phase II. The technical details are provided in the Technical Approach section below.

B. Technical Approach

The technical approach that was used in Phase I was to evaluate possible versions of microtron designs and parameters to produce a conceptual design and select an optimal set of components and parameters

for a prototype. Starting from the basic concepts of the microtron, we examined and analyzed the characteristics of microtrons that were developed in the past, including microtrons that were designed and developed by one of our team members, we produced a conceptual design and selected an optimal set of parameters for a prototype. We evaluated three different magnet designs, permanent, electromagnet, and hybrid that used both a permanent magnet and correction coils. Our technical approach utilized the extensive microtron experience of our chief designer, Dr. Grigory Kazakevich, who led the design and development of a compact microtron that was successfully built as an injector to a free electron laser in South Korea. We developed our conceptual design by considering the characteristics of the Korean microtron and adapted or changed the parameters and components to meet the objectives of our project. We have included references to publications from the Korean microtron to not only point to their technical material but to show that our team has the expertise and knowledge to be successful in this project. The prototype is designed to provide high performance, low fabrication and maintenance costs, and will serve as a basis for several commercial versions. The major components of the microtron system are the acceleration cavity and associated RF subsystem, the electron source and injection subsystem, the combined magnet and vacuum system subsystem, the beam extraction subsystem, and the measurement and control subsystem. In this section, we will describe the subsystems of the prototype microtron system and show the results of our analysis of the parameters and the performance expectations.

1. Principles of the microtron

Microtrons were conceived of and developed primarily outside the USA, mainly in Russia.
The original concept was by Veksler [1]. The classic microtron, illustrated in **Error! Reference source not found.**, is a circular electron accelerator in which the magnetic field is fixed and uniform. Acceleration is provided by a single RF cavity inside the circular magnetic field region.

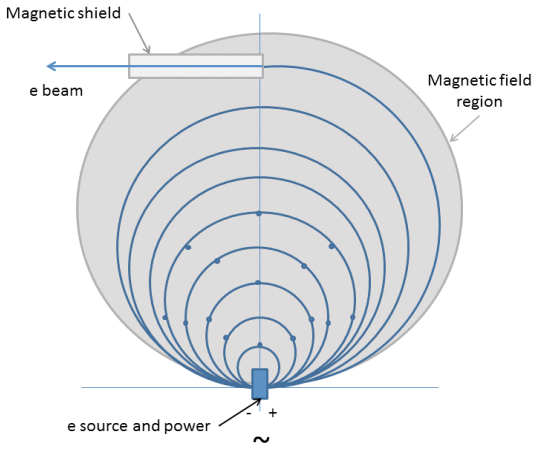

Figure 1: Simplified representation of a classic microtron. The source of electrons is a heated cathode within an injector. The acceleration is provided by a single RF cavity co-located with the source. Resonant acceleration is achieved when the circumference of each successive orbit increases by an integral number of RF wavelengths. Electrons can be extracted tangentially to the final orbit by means of a magnetically shielded tube, as shown. Alternatively, internal targets can be placed in the beam.

The RF frequency is the most significant design parameter, as it sets the scale for the accelerating system, the injection system, and the magnet. Three RF frequency bands (X-band 8-12 GHz, C-band 4-8 GHz, and S-band 2-4 GHz) have been studied in Phase I, and S-band was selected for the prototype. Type I and Type II injectors were studied, and Type II was selected. Three different magnet types: permanent,

electromagnet, and permanent with correction coils were studied, and the electromagnet was selected for the prototype. The studies are included in this Phase I Final Report.

2. Design and operation of the microtron

The classic microtron is a circular electron accelerator in which the magnetic field is fixed and uniform, and acceleration is provided by a single RF cavity inside the magnet. The beam energy and radius increase with each pass through the RF cavity gap. The microtron is based on a Principle of Resonant Acceleration first proposed and developed by V. Veksler [1].

According to this principle each particle bunch passes through the accelerating gap of the RF cavity at the same (resonant) phase of the accelerating RF field. Each pass of the electron bunch through the accelerating gap produces an increase in energy, [2].

$$\Delta W_S = eV_a \frac{\sin(\theta/2)}{\theta/2}\cos\varphi_S \qquad (1)$$

where V_a is the amplitude of the accelerating voltage, θ is the so-called phase angle and $\varphi_S \approx 17$ deg. is the equilibrium synchronous phase. For relativistic particles $\theta/2=\pi d/\lambda$, where d is the accelerating gap width, λ is the wavelength of the RF voltage, $l=d/\lambda$ is the (dimensionless) length of the accelerating gap in λ units. Thus for microtrons $\Delta W_S = eV_S$ and V_S is the resonant accelerating voltage. The period of revolution of the electron with total energy U in a magnetic field H is

$$T = \frac{2\pi U}{ecH}, \quad (U=W+m_0c^2). \qquad (2)$$

Since the energy of the resonant electron after passage across the accelerating gap increases each time by exactly the same value $\Delta W_S=\Delta U = eV_S$, the period of revolution of the electron also increases each time by the same amount $\Delta T = T_{n+1} - T_n = \frac{2\pi \cdot \Delta U}{ecH} = T_0$. Here n=1, 2, …is the number of the passages through the RF cavity. This fact is precisely the basic idea of the microtron. Although the period of rotation of the accelerated electron increases from turn to turn, while the period of the accelerating field does not change, nevertheless one can maintain resonant acceleration of the electron with a constant resonant phase. Denoting H_c the "cyclotron" magnetic field in which period of revolution of electron with the total energy of m_0c^2 (its rest energy) is equal to period of the accelerating field, $T_a=2\pi/\omega_a$, *i.e.*, $H_C = \frac{m_0c^2 \cdot \omega_a}{ec} = \frac{2\pi \cdot m_0c^2}{e \cdot \lambda}$. Then the increment of the energy of electron conserving the synchronism with the accelerating field at the same RF angular frequency ω_a is $\Delta U/U = H/H_C = \Omega$. The total energy on the nth orbit of the microtron is expressed as:

$$U_n = (n-1)\Omega \cdot m_0c^2 + U_1. \qquad (3)$$

Here U_1 is total energy of electron on the first orbit passing through the accelerating cavity. For synchronism it follows that total time of motion of electrons on the n^{th} orbit, t_n, takes the following integral number of periods: $t_n/T_0 = (n-1+m)$, in which m is an integer. Then

$$U_n=(n+m-1)\Omega \cdot m_0c^2. \qquad (4)$$

Comparing Eqs. (3) and (4) one obtains

$$U_1=m\Omega \cdot m_0c^2 \text{ and the } \Omega_{min}=1/m.$$

Since the minimum value of $T_1=2T_0$, the $m_{min}=2$. The accelerated electrons in a microtron are relativistic, thus the diameter D_n of the n^{th} orbit is:

$$D_n = (n+m-1) \cdot \lambda/\pi. \qquad (5)$$

Since the period of revolution of the electron in a microtron is inversely proportional to the magnetic field, H, Eq. (2), at the given λ and the given energy the diameter of the n^{th} orbit, D_n, is inversely

proportional to H. In designed or operating microtrons, $H \leq 0.3$ T, unlike the betatrons, where H is typically 0.5 T to 1 T. Thus, the diameter of the microtron chamber at the given energy will be larger than that of the betatron. Therefore, although microtrons can't be more compact than betatrons at the same energy, microtrons provide much higher dose rates than betatrons at the same energy. In addition, microtrons are capable of extraction of beam practically without losses due to the low energy spread of the beam and the good separation of adjacent orbits at the extraction points, as shown in **Error! Reference source not found.**.

The proposed microtron applicable as a highly intense source of bremsstrahlung for scanning radiography and an intense source of photo-neutrons for detection of fission or/and explosive materials is limited by the electron total energy of 9.5 MeV. It allows avoidance of the photo-neutron activation of the microtron components providing safe maintenance of the accelerator.

The analysis of the parameters and the features of the proposed 9.5 MeV compact microtron presented in this document will be attractive to a variety of users.

3. Definitions of microtron parameters and performance estimates

In this section, we provide definitions of the parameters and discuss the inter-relationships between the parameters. To satisfy the conditions of the principle of resonant acceleration, there are integer parameters, n and m, which are the number of orbits in the microtron and the number of periods that the accelerating field needs for the electron circulation along the first orbit. The parameter Ω, defined as H/H_C, where H is the magnetic field in the microtron, and H_C is the cyclotron magnetic field, in which period of revolution of electron with the total energy of m_0c^2 (its energy of rest) is equal to period of the accelerating field, $T_a=2\pi/\omega_a$.

For synchronicity, the fractional increase in electron total energy is $\Delta U/U = H/H_C = \Omega$. The integer parameter m, determines the length and dimension of the first orbit that completely encircles the cavity. The minimum value of m is 2, and two important relations involving n, and m, are the following: $U_n=(n+m-1)\Omega \cdot m_0c^2$ for the total energy of the n^{th} orbit electrons, and $D_n = (n+m-1)\cdot\lambda/\pi$.
D_n is the diameter of the n^{th} orbit and λ is the wavelength of the accelerating field. These relations will be used in the following sections.

We present computations for microtrons with 6.5 MeV as well as 9.5 MeV total electron energy. We have analyzed using S-band, C-band, and X-band RF frequencies (discussed below), and have selected S-band for the Phase II prototype. The compact S-band microtron prototype can deliver additional output capabilities if the energy is increased from 6.5 MeV to 9-10 MeV. Table 1 shows the computed characteristics and parameters for an S-band compact 9.5 MeV microtron with Type-II internal injection and a cathode emitter diameter, D_C=2.5 mm. $D_{Pole} = D_n+\lambda$ is the diameter of the magnet pole, I_n is the pulsed beam current in the n-th orbit, P_{RF} is the pulsed RF power, t_{Cath} is the cathode lifetime and c_n is the capture coefficient for n-th orbit.

Note that the estimated E_0 for the S-band accelerating cavity is about 41 MV/m, which will operate with greater reliability for users. Extraction of the electron beam at various energies can also be implemented on this microtron.

Table 1: Computed characteristics of a 10-orbit S-band 9.5 MeV compact microtron with Type-II injection

U_n, MeV	n	D_n (m)	D_{Pole} (m)	I_n (mA)	Ω	c_n (%)	P_{RF} (MW)	i_C (A/cm^2)	Cathode	t_{Cath} (h)	Gamma Dose (R/min·m)
9.5	10	0.375	0.482	65	1.8	4–5	2.0	28.4	LaB_6	>1000	1778

An S-band microtron with total energy increased from 6.5 MeV to 9.5 MeV and beam extraction can provide an intense source of neutrons by utilizing an external U-Be target. This combined target allows the most effective conversion of energy of electrons to bremsstrahlung with a consequent (γ, n) reaction on nuclei of Be and U. The choice of the total energy significantly less than 11 MeV allows avoidance of photo-neutron activation of the microtron components (accelerating cavity, where the threshold of (γ, n) reaction is about of 10.6 MeV) providing safe maintenance of the accelerator. The photo-neutron yield is about $6 \cdot 10^{10}$ n/s [2] for 9.5 MeV total electron energy. 65 mA pulsed beam current, 1/1000 duty factor (the average beam power is ≈585 W), and optimized U-Be target. The estimated gamma dose and neutron dose are derived from the graphs in Figure 2, using 65μA average current (average current I_n, 65mA from Table 1, multiplied by the duty factor, ~0.001).

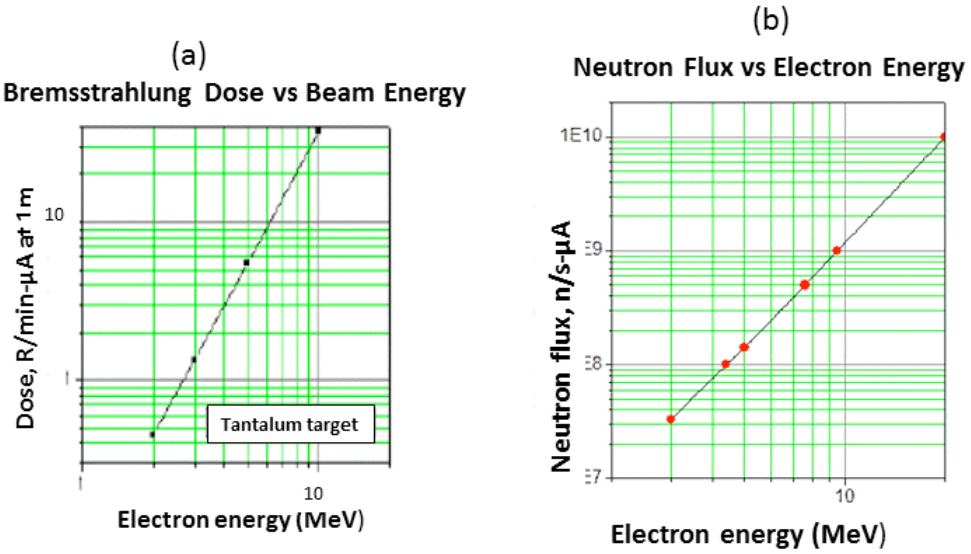

Figure 2: (a) Gamma dose vs electron energy, (b) neutron flux vs electron energy, from [2]

The neutrons can be used for detection of explosive materials, fission materials and other applications. These estimates show that the S-band microtron with Type-II injection design provides high beam power, gamma production, longer cathode lifetime in comparison to the C-band and X-band microtrons analyzed in the Phase I Final Report. Furthermore, the 9.5 MeV S-band microtron can produce significant neutron production rates by using an appropriate target.

4. Microtron accelerating system

Accelerating systems of the compact microtrons are usually based on a cylindrical accelerating pillbox cavity with a thermionic cathode [2], or (rarely) with a rectangular pillbox [3]. In both cases Ω can be chosen from 0.8 to 2, depending on the injection scheme. The cylindrical RF cavity is easier in manufacturing; we will use it in the prototype.

The accelerating cavity of a microtron is usually fed by a relatively inexpensive pulsed magnetron auto-generator with respective wavelength and power via ferrite circulators or ferrite isolators. The power of the generator is determined mainly by losses in the accelerating cavity and the required power of the accelerated beam. For the cylindrical RF pillbox cavity the power loss is estimated as in [3] by:

$$P_r \sim \frac{1.02}{2\pi}\sqrt{\frac{c}{\lambda\sigma}}\left(1.2+\arcsin\frac{1}{1.88\varepsilon}\right)\varepsilon^2\Omega^2 P_0. \qquad (6)$$

Here σ is conductance of metal of the cavity, $\varepsilon=E/H$ characterizes the accelerating field, and P_0=8700 MW is the characteristic electron power. Note that an increase of Ω decreases size of the microtron magnet but notable increases the power lost in the cavity walls requiring more powerful RF source. In accordance with Ref. [3] the following parameters of the microtron prototype were chosen to provide compactness and large beam intensity: U_n=9.5 MeV, n=10, Ω=1.8. ε=0.8. Assuming utilization of a 2 MW S-band magnetron and losses in the RF system, P_{Loss} ≤1 dB, including losses in ferrite circulator, waveguide window, waveguide line, as it is presented in [3], and power loss in the cavity, P_r, one can estimate RF power utilized for acceleration, P_{Acc}:

$$P_{Acc}=2\text{ MW}-P_{Loss}-P_r\approx 1.175\text{ MW}.$$

Since in microtrons about half of the RF power absorb the non-resonant electrons, i.e., the efficiency of acceleration, $\eta_n\approx 0.5$, [3], the pulsed power of the accelerated beam, P_n, is:

$$P_n\approx P_{Acc}\cdot\eta_n\approx 588\text{ kW}.$$

This allows to calculate the required coupling coefficient of the accelerating cavity, β, [3]:

$$\beta=\frac{P_n}{\eta_n\cdot P_r}+1\cong 3.85.$$

Then the pulsed accelerated maximum current of the microtron is determined as:

$$I_n\approx P_n/(U_n-m_0c^2)\approx 65\text{ mA}.$$

5. Microtron RF Power system

The compact microtron RF system is powered by a pulsed magnetron [3] that provides the required frequency and power. A conceptual schematic of the microtron RF system is shown in Figure 3. The magnetron is coupled to the accelerating cavity via a waveguide system that includes a ferrite circulator with a matched load, a directional coupler and the waveguide vacuum window. The circulator with the matched load provides stable operation of the magnetron preventing discharges caused by a reflected wave. At the circulator inverse loss of 17-20 dB the magnitude of the reflected wave passing towards the magnetron is enough to stabilize the magnetron frequency, making the generation frequency-locked by the reflected wave, [5]. The directional coupler allows observation and measurement of the forward and reflected waves. This allows choosing the regimes of powering the cavity by the magnetron and optimizing operation of the RF system. The waveguide vacuum window separates vacuum in the cavity and the dielectric gas (SF_6) filling the waveguide system to protect it from discharging due to the high RF power in the system. Because of the high RF power feeding the accelerating cavity, the cavity and the matched load have to be cooled by water. Water cooling is also required for anode in high-power magnetrons.

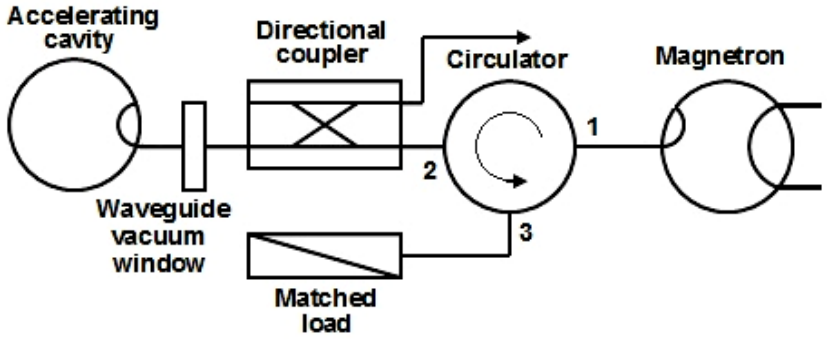

Figure 3: **Schematic of the microtron RF system**

An example of the design of an RF system used in a variable-energy microtron built by Kazakevich, et al [3] is shown in Figure 4. The RF system is mounted on a moving stage, which allows changing the orbit number of the final orbit by moving the accelerating cavity relative to the fixed extracting channel, thus changing the beam energy. The RF system is mounted on a moving stage, which allows changing the number of the final orbit by moving the accelerating cavity relative to the fixed extracting channel, thus changing the beam energy.

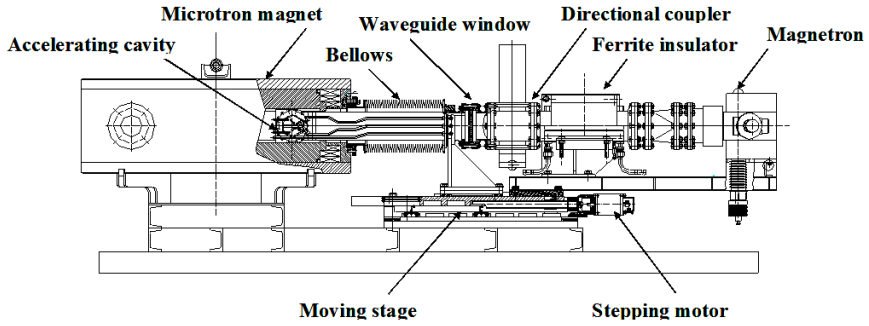

Figure 4: Layout of the RF system of a variable-energy microtron, reprinted from [5]

6. The microtron injection system

The function of the microtron injection subsystem is to provide the high current densities of emitted current required by the user applications, while being compact, inexpensive and reliable. Reliability is limited by the cathode lifetime, which depends on the cathode material and the operational temperature. A detailed analysis of the internal injection by Kazakevich is presented in [4]. Since injection in microtrons occurs in a high gradient RF field (~10 MV/m and more) only LaB_6 crystals or pure metals (W, Ta) can be used as emitters. We will use single-crystal LaB_6 cathodes for operation of the prototype at high current densities. Due to the Schottky effect, field emission supplements thermionic emission, so that the necessary current density can be provided at lower temperatures, allowing cathode life times to be ~ 1000 h or more with much-reduced erosion of the cathode (c.f. [4]). Electrons are injected in a resonant phase and accelerated by the high gradient RF field. Injection efficiencies up to 3% to 5 % can be attained and high current density of the emitted beam can be achieved. The lifetimes of pure metal cathodes (10 to 20 h) are acceptable for demonstration of proof-of-principles or experimental modeling of the microtron features, but are not long enough for most user applications.

Two internal injection geometries, Type-I and Type-II [2], were studied in Phase I to provide the necessary emission and acceleration currents. Type-I is shown in Figure 5. For the S-band prototype, Type-II was chosen for the injection mode. A Type-II injector similar to that shown in Figure 6 will be designed for the prototype.

Microtrons intended for user applications utilize compact, inexpensive and reliable type-II internal injection system, [3], to provide the necessary emission and accelerated currents. The electrons are injected in a resonant phase and accelerated by a high gradient RF field. Injection efficiencies up to 3% to 5 % can be attained and the high current density of the emitted current can be achieved without significant overheating of the cathode due to field emission by the Schottky effect. Trajectories of injected electrons for the type-II injections are presented in Figure 6. Note that electrons emitted from the cathode which to not enter the proper trajectory are not shown; they are quickly removed by hitting a wall at low energy.

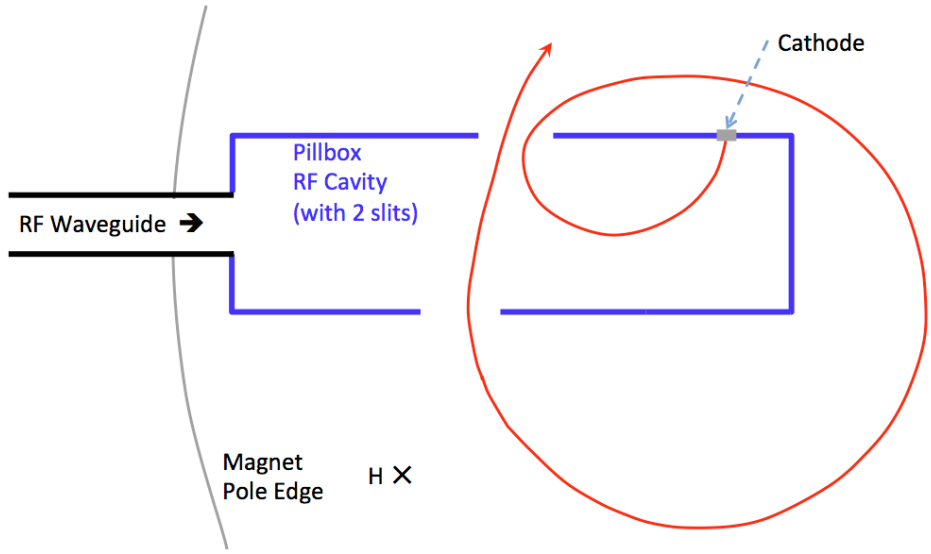

Figure 5 Initial trajectories of resonant electrons in a microtron using Type-I internal injection, redrawn from reference [Error! Bookmark not defined.**]. In Type I injection, electrons emitted from the cathode pass through one of the two larger slits before assuming the paths taken by the successive orbits through the cavity.**

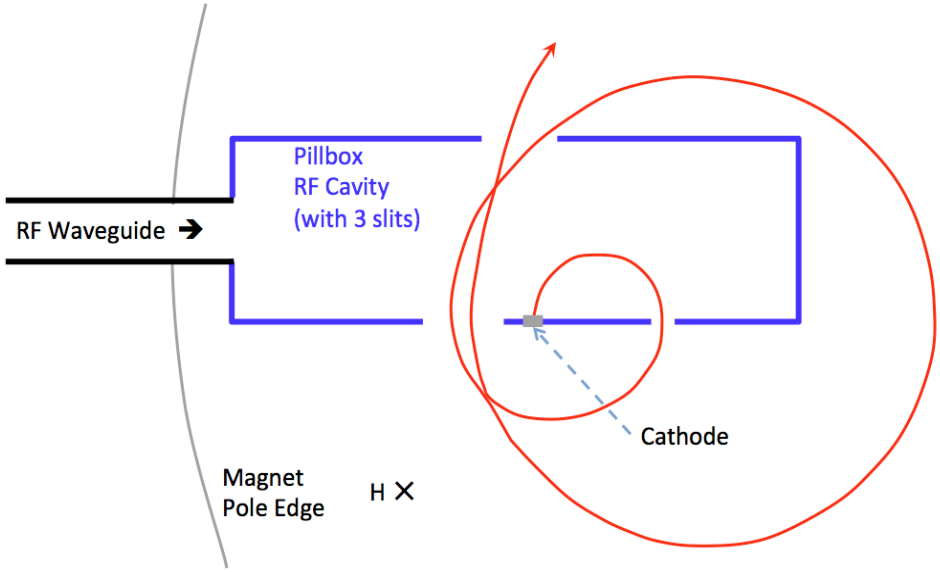

Figure 6: Initial trajectories of resonant electrons in a microtron using Type-II internal injection, redrawn from reference [Error! Bookmark not defined.**]. In Type II injection, electrons emitted from the cathode, located near the symmetry axis of the flat-walled cylindrical cavity, pass through a small slit in the cavity wall, and make one revolution through the two larger slits before assuming the paths taken by the successive orbits through the cavity.**

As it is shown in Figure 6, the type-II injection scheme utilizes an additional radial slit in the median plane in the cavity cover for passage of the electrons along the first orbit. In so called type-II injection scheme, Ω can be ~2 this allows increase the magnetic field decreasing diameter of the magnet.

A detailed analysis of the internal injection is presented in [4]. Since the injection in microtrons occurs at a high gradient of the RF field (>10 MV/m) only LaB_6 crystals or pure metals (W, Ta) can be used as emitters. We will consider only single-crystal LaB_6 cathodes. They provide the necessary current density at the temperatures allowing cathode life times to be ~ 1000 h or more. The lifetime of pure metal cathodes (~ 10-20 h) are acceptable for demonstration of proof-of-principles or experimental modeling of the microtron features, but are not long enough for user applications.

The cavity except a hole for injector (and an additional slit for passage along the first orbit in the type-II injection scheme) has two radial narrow slits for passage of the accelerated electrons; the emission surface is recessed in a hole below the internal surface of the pillbox. The hole for the recessed emitter acts like a lens and provides some focusing of the injected electrons. For a hole of radius r_H and a recession depth d_C the RF field in the cathode surface center is, from [4]:

$$E_{CS} \cong E_0 \cdot J_0\left(k_0 \cdot R_C\right) \cdot \cos(\varphi_S) \cdot J_0\left(k_r, r\right) / \cosh\left(k_z \cdot d_C\right) \tag{7}$$

Here $E_0 = \dfrac{\Omega m_0 c^2 \cdot (\theta/2)}{e \cdot l \cdot \sin(\theta/2) \cdot \cos\varphi_S}$ is maximum field on the cavity axis determined by Eq. (1), l is the cavity length, J_0 is the Bessel function of the first kind, $k_r = \chi_{01} / r_H$, where $\chi_{01} = 2.405$ is the first zero of the Bessel function and $k_Z = \sqrt{k_r^2 - k_0^2}$. Considering the Schottky effect one can express the current density of a LaB_6 single crystal emitter as a function of (r, φ) as:

$$i_C(T, r, \varphi) = AT^2 \cdot \exp\left[\frac{-e\phi_C + 3.79 \cdot 10^{-4} \cdot \sqrt{E_{CS}(r, \varphi) \cdot 10^6}}{k \cdot T}\right]. \tag{8}$$

Here: A=73 A / K^2cm^2 and $e\phi_C = 2.66$ eV are the Richardson constant and the work function for LaB_6, respectively, k is the Boltzmann constant and T is the emitter temperature in Kelvin. Then the initial value of the emission current at the emitter radius of r_C should be equal to, [4]:

$$I_C(T) = \int_0^{2\pi r_C} \int_0 i_C(T, r, \varphi) \cdot r \, dr \, d\varphi. \tag{9}$$

Equations. (8), (9) allow quite accurate computations of the current density at the given location of the emitting surface in the RF cavity at the given strength of the accelerating field on the cavity axis and the temperature of the emitting surface.

Note that some part of electrons emitted in non-resonant phases back-stream to the emitting surface and additionally heat the cathode. This results in an increase of the emission current along the RF pulse. For an RF pulse duration ≤ 2 μs this effect can be neglected in the first approximation.

Internal injection with thermionic cathodes allows easy control of the accelerated current from 0 to maximum by varying the injector filament current.

Compact microtrons have used various cathode designs with both direct and indirect heaters ([3], [4]). Cathodes with indirect heaters [ibid] achieve longer lifetimes. A precisely-stable, indirectly heated cathode design as shown in Figure 7 was developed and used in an S-band microtron, [4].

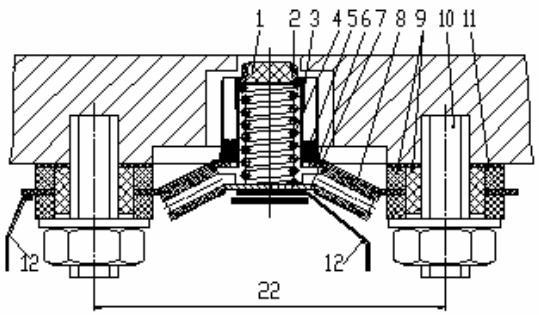

Figure 7: Layout of the microtron cathode assembly developed in Ref [4] (1) emitter, (2) graphite holder, (3) cathode sleeve, (4) cylindrical filament, (5) heat shields, (6) carrying base, (7) tantalum plate, (8) ceramic insulators, (9) ceramic insulators, (10) titanium studs, (12) wire lead, reprinted from [4].

The cathode uses a 2.5 mm diameter [100]-face LaB_6 single crystal tablet-shape emitter It is fixed in the graphite holder, (2), with an outside diameter of 3 mm. The emitter thickness is 1.1 mm. The graphite holder prevents diffusion of boron into the tantalum components of the assembly; which significantly increases the assembly lifetime.

The cathode sleeve, (3), is welded with a precisely fitted mount to the base, (6), whose width and thickness are 7 mm and 0.3 mm, respectively. The cylindrical filament, (4), is made from 0.5 mm diameter tungsten wire and consists of 8.5 turns with a 0.75-mm step. The cathode sleeve is surrounded with 8 heat shields, (5), providing considerable reduction of heat losses through the sidewalls of the heater chamber. This decreases the filament temperature and noticeably increases lifetime of the filament.

The cathode provides emission current up to 1.3 A with a life time of 1000 h limited by evaporation of the LaB_6 tablet. The microtron with this cathode is used for about 15 years in the S-band microtron with type-I injection scheme. The developed cathode can be used for microtron with type-II injection scheme after decrease sizes of the heat shields and carrying base. For microtrons with type-II injection one can use also an indirectly heated injector such as shown in 6.

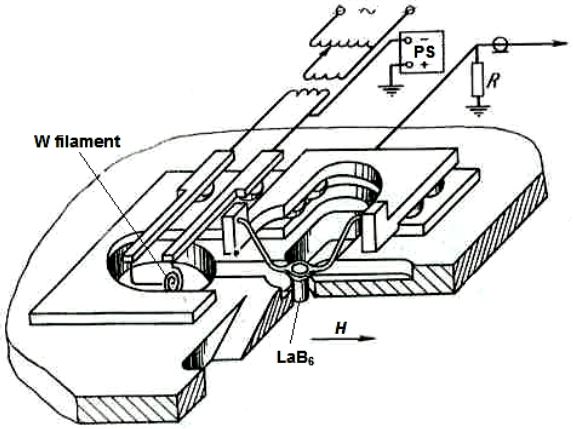

Figure 8: LaB6 cathode heated by a beam, reprinted from Reference [3]

In this cathode the single crystal LaB_6 cylindrical cathode mounted on the RF cavity cover is heated by an electron beam emitted by a W filament. The beam passes along the magnetic field *H* of the microtron. The cathode may provide emission current up to a few A at the life time in hundreds of hours [3]. The cathode emitting surface is located at almost the maximum of the electric field of the RF cavity, thus the Schottky effect significantly increases the emitted current density and the emitted current at a lower

temperature as shown by Eqs. (8), (9) in Section IV.B.6. The required cathode temperature vs. the emitted current is determined by Eqs. (8) and (9).

The injection parameters for S-band Type-II injection are shown in E0, in which I_n/k_n is the ratio of current in the n^{th} orbit to the capture coefficient for this orbit, c, Ω is defined in Table 2. Here D_c is the diameter of the cathode, E_0 is the acceleration field on the cavity axis, E_C is the electric field at the cathode center, i_C is the current density at the cathode, and I_C is the cathode current.

Table 2: Injection parameters for type-II S-band microtrons

Microtron, injection	I_n/k_n, A	Ω	$2r_C$, mm	E_0, MV/m	E_{CS}, MV/m	i_C, A/cm^2	I_C, A
S-band, type-II	1.778	1.8	2.5	40.7	32.4	55.6	2.23

In the S-band microtron with the type-II injection has $I_n/k_n<I_C$; this means that the cathode temperature can be decreased, which further increases the cathode lifetime.

7. Description of the magnet-vacuum system

The microtron magnet provides the field to keep the electrons on their circular orbits. The size of the magnet will have a large impact on the mass of the system. The magnetic field must be uniform with field non-uniformity $\Delta H/H$ less than $\sim 1/n^2$ where n is the number of orbits in the microtron. In addition to the primary function of providing the magnetic field, the magnet can provide the enclosure of the vacuum system, which eliminates the need for a separate vacuum chamber inside the magnet. The combined magnetic-vacuum system is sealed by an indium wire between the upper and lower poles of the magnet, Ref. [6]. The chamber-less magnetic-vacuum system of the microtron demonstrated convenience in operation and maintenance, good vacuum features and good reliability during more than 15 years of operation.

We have examined three alternative magnet types for a 6 MeV compact microtron gamma source. These include (1) a magnet using permanent magnet material instead of coils to provide the field, (2) a hybrid magnet where the dominant part of the field comes from permanent magnet material, but trim coils are used to provide some variation of the magnet field for tuning, and (3) a magnet with copper coils around the iron magnet poles. Each of these approaches has some advantages and some disadvantages which will be discussed in a report presented in Ref. [10]. We have chosen to pursue an electromagnet with copper coils for our proposal. Using coils allows greater flexibility. The magnet field could be varied to allow tuning to keep the resonant condition for the microtron. It could also be used to change the output energy by varying the magnetic field and power of the magnetron.

To allow usage of the proposed compact microtron as a source of gamma-radiation and neutrons we consider the tubeless magnetic-vacuum system of the S-band 9.5 MeV microtron with type II injection. The engineering estimates for the microtron magnet were performed for 10 turns with a field B_y=1800 gauss (Ω=1.8) and a 2.8 GHz RF frequency (λ =0.107 m) and maximum magnetic induction in the magnet yoke, B_{max} =1.3 T. The vacuum sealing is provided by Indium wire with diameter of 1.0 mm. A schematic of the generic microtron is shown in Figure 9.

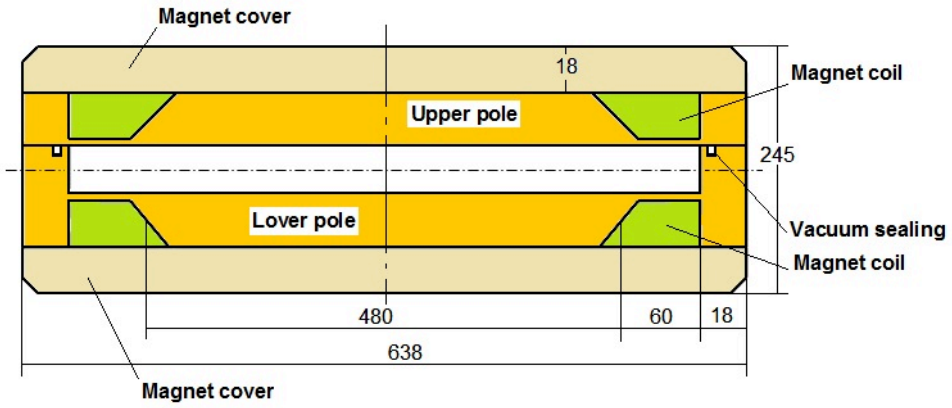

Figure 9: Sketch of the 9.5 MeV tubeless generic microtron vacuum-magnetic system. All sizes are in mm.

The initial engineering estimates for the design parameters of the proposed magnetic system gave *In≈7650* A-turns for each coil, the current density in the coils, $i_c \approx 3\ A/mm^2$, and the power lost in the both coils, $P_c \approx 1790\ W$ at the required magnetic field.

Optimization of the magnets design was performed using the simulation software "Opera". Applying the finite element analysis to the generic sketch for various wavelength of microtron we found the adjustments allowing decrease a saturation of the iron yoke around the coils in order to reduce the mass of the magnet. The optimized design of the microtron magnet is reflected in Table 3.

Table 3: Parameters to describe the electromagnet geometry for a 9.5 MeV microtron

Symbol	Parameter Description	Units	S-Band II
H	Magnetic Field	T	0.18
R_{pole}	Mean Inner Coil Radius	mm	241
h_r	Flux Return Width	mm	26
h_y	Upper Yoke Height	mm	26
h_{pole}	Height of Pole and Coil	mm	59
R_{yoke}	Outer Yoke Radius	mm	326
In	A·turns /per a coil	A·turns	9234
J	Current Density	A/mm^2	2.85
A_{coil}	Coil Cross Section Area	mm^2	3763
h_{coil}	Coil Height	mm	54
b_{coil}	Coil Width	mm	60
h_{web}	Height of Coil Web	mm	5
W	Total Magnet Mass for Fig. 4.3 Design	kg	409
W'	Magnet Mass with Iron Removed	kg	339

Analysis of the field distribution in the yoke shows that the center part of the flux return hat is not saturated. It allowed removing of part of the top hat, reducing the magnet weight by 70.4 kg at the same field performance. Note that a decrease of the required current density allows using air or a low water flow for cooling of the adjusted magnet. **Figure 10** shows a proper shaping the field profile reducing of non-uniformity of the magnetic field. The optimization with the simulation improves the magnetic field non-uniformity and minimize the weight of the magnetic system.

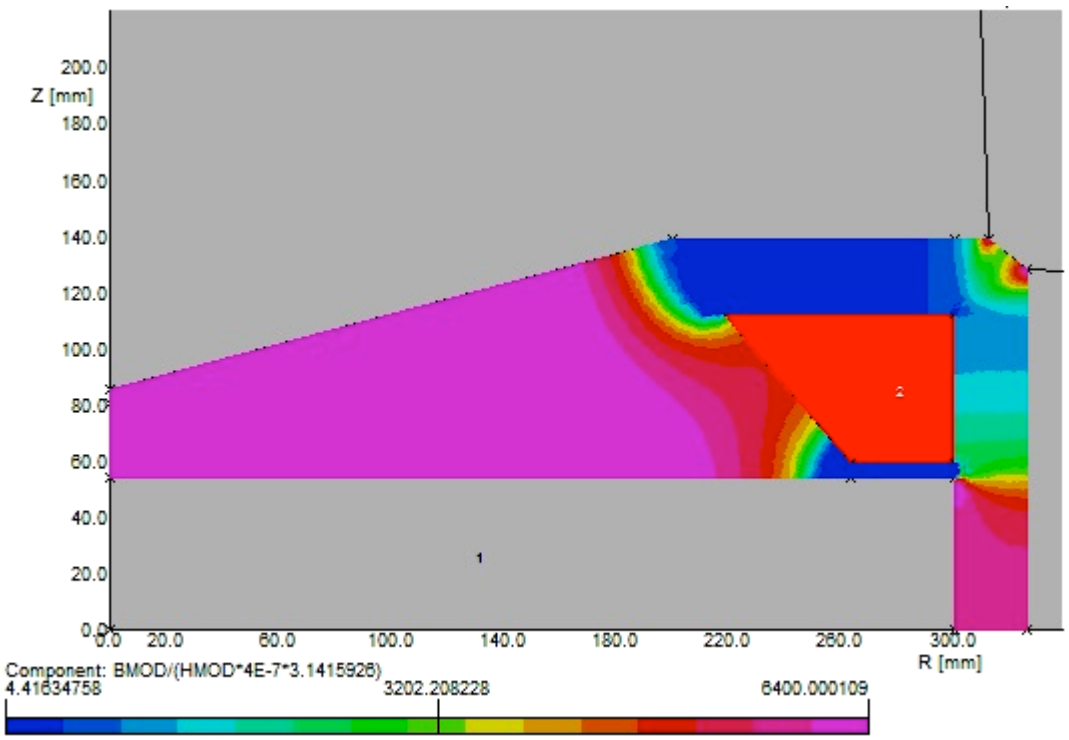

Figure 10: Distribution of the magnetic field in the optimized S-band 9.5 MeV microtron magnet.

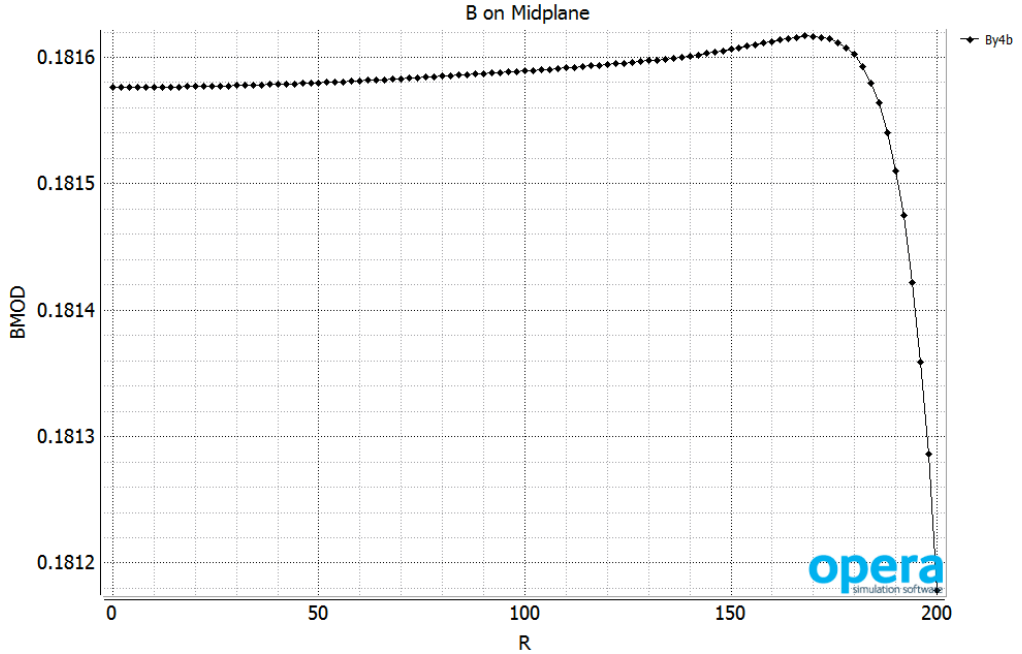

Figure 11: Optimized magnetic field profile

8. Description of the microtron beam extraction system

The electron beam can be extracted passively by installing a tube of soft steel inside the main magnet at a tangent to the circular trajectory at the final orbit such the beam exits along the tangent. The magnetic field is perturbed by the presence of the extraction tube. The field non-uniformity would perturb the previous beam orbits. A scheme similar to the type used in Reference [6] is illustrated in Figure 12 and will be employed to suppress the field non-uniformity. Choosing diameter d of the compensating rods made from soft steel and distance δ it was possible to optimize the extracting system for a high efficiency of the beam extraction as it is shown in Figure 13. The task will be simulated using software "Opera"

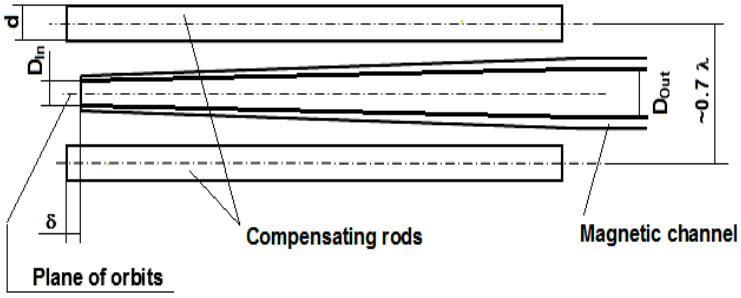

Figure 12: The extracting system of 12-orbits S-band microtron

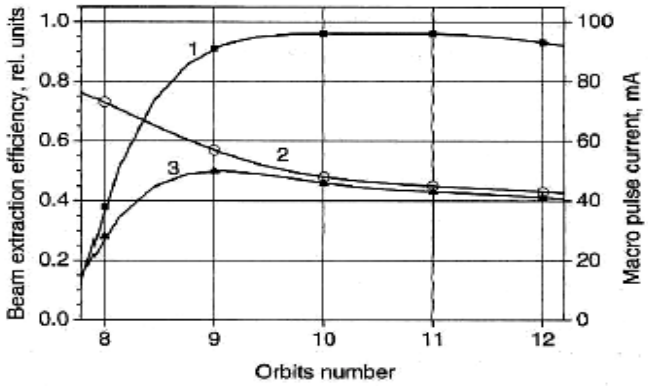

Figure 13: Beam extraction efficiency and the beam currents as functions of the orbit number at a constant loading of the RF cavity. l- electron beam extraction efficiency (left scale); 2- accelerated macro-pulse current (right scale); 3- the macropulse current extracted into the beamline (right scale).

9. Description of the control system

The control system includes an interface of all the microtron system with a computer and the interlock system allowing some functions in automatic regime. The simplified schematic of the control system for the microtron is shown in Figure 14.

The control system provides necessary stability of the microtron magnet current, the cathode filament voltage, the cathode filament bias voltage, the cathode emission current, allows required positioning of the extracting channel or the RF cavity and measurements of the target current. The interlock as a part of Graphical User Interface (GUI), *e.g.*, created by LabVIEW provides safe operation of the microtron at the required vacuum, cooling water flows for the accelerating cavity, microtron magnet, magnetron anode and beam target. The interlock provides safe operation at closed shielding.

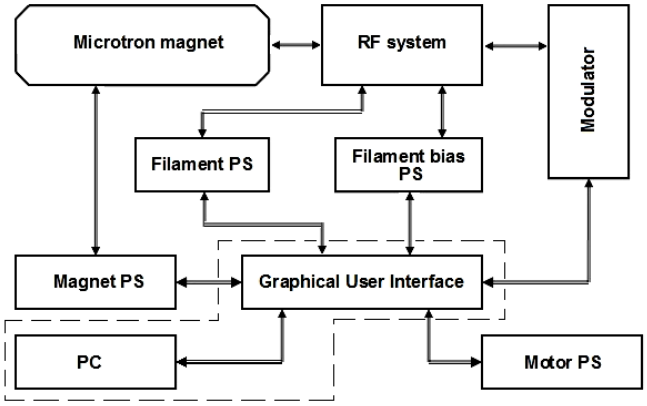

Figure 14: Schematic of the control system

10. Analysis of X-band, C-band and S-band compact microtrons

Of the many parameters that need to be determined for the microtron, the choice of accelerating frequency has the most impact on the design of the microtron. The size scale depends directly on the wavelength, which affects capability of reliable work, the magnet size, the dimensions of the injector, and the size and type of the injector.

a) X-band microtrons

Our initial goal, to build the smallest sized microtron, led us to study the X-band microtron because the wavelength (~3.2 cm) is smaller than those of the C-band (~5 cm) and S-band (~10 cm) microtrons, and the size of the final orbit of an X-band microtron for a given energy is theoretically the smallest. However, this analysis shows some of the problems in producing a high-performing X-band microtron.

As an example, the first X-Band microtron with an internal injection by a thermionic cathode was described in [8]. This 18-orbit microtron had a vacuum chamber with inner diameter of 255 mm inside a cylindrical, closed electromagnet that produced a low magnetic field inhomogeneity of ≈0.28% over 85% of the pole diameter. It utilized a 9.3 GHz 240 kW pulsed magnetron, which provided at the 18^{th} orbit, 2 mA pulsed accelerating current with pulse duration of 1 μs at total energy 5.8 MeV and $\Omega \approx 0.62$. The lower value of Ω with the internal injection allowed a decrease the accelerating field in the RF cavity to ~ 50 MV/m for reliable operation of the microtron. A thermionic tantalum cathode 0.7 x 0.7 mm^2 was mounted on the inside wall of the cylindrical TM_{010} mode accelerating cavity, and it provided the emission current of ~150 mA at a capture coefficient $k_n \approx 1.3\%$ at n=18. The microtron injector used m=3 with an additional path of the electrons in the first orbit (like the type-II injector, in which usually m=2).

Another X-band microtron was the 13-orbit microtron described in Reference [9]. It used a magnetron of power 200 kW, and it provided a total energy of 4.3 MeV, an accelerated current of 1.5 mA, and used the same type of internal injection as was used in Reference [9]. The weight of the electromagnet was ~100 kG. Subsequently the microtron was improved and carefully tuned. With a 240 kW magnetron, it provided an accelerated pulsed current up to 10 mA and an average current up to 9 μA on the last orbit. The microtron provided dose power up to 27 R/min·m with Tantalum target 0.3 rad. units thick and was used to determine the beryllium concentration in geological samples by the photo-neutron method.

These X-Band microtrons provided currents and doses of gamma-radiation that were a few times higher than compact betatrons, but required quite high RF gradients in the cavity and very high densities of the emission current because of small sizes of the emitting surface. These requirements limit reliability of operation of this type of accelerator in industrial applications. By decreasing the accelerating field in these versions injection in a lower magnetic field required a greater number of orbits to reach the same final energy. This results in a larger vacuum chamber diameter (inversely proportional to Ω) and a large

increase in the weight of the microtron magnet. Moreover, the increased number of orbits, n, requires a much lower inhomogeneity of the magnetic field as $\Delta H/H \approx n^{-2}$.

Other serious problems with the described X-band microtrons are the relatively low capture coefficients at m=3 and short cathode lifetimes, t_{Cath}. The short cathode lifetime results from the high density of the emitter current resulting from the need to use small cathodes (~ 0.7 x 0.7 x 3 mm^3 or less), which limits the cathodes to be metallic (W, Ta) and precludes the use of LaB_6 cathodes. To produce the high emitter currents needed, the metallic cathodes must operate at high temperatures, which limit the lifetimes to ~10-20 hours. For larger RF wavelengths such as used in S-band microtrons, the cathode sizes are correspondingly larger and LaB_6 emitters can be used, which operate at significantly lower temperatures and have much longer (~1000 h) lifetimes at higher capture efficiencies at m=2 .

The following is a summary of the parameters and characteristics of the two previously built X-band microtrons described above and the calculated parameters for an X-band microtron that is applicable for use as a gamma source that can produce gamma rays up to ~6 MeV. Table 4 lists the parameters of the two previously built X-band microtrons.

Table 4: Technical characteristics of the two previously built X-band compact microtrons

Ref.	U_n, MeV	n	D_n, m	D_{Pole}, m	$I_{n,}$ mA	Ω	k_n, %	P_{RF}, MW	i_C, A/cm^2	Cathode material	t_{Cath}, h	Dose power, R/min·m
[8]	5.8	18	0.204	>0.285	2.0	0.62	1.3	0.240	30.6	Ta	~10	12.4
[9]	4.3	13	0.153	0.210	1.5	0.61	1.2	0.200	25.5	Ta	10	4.1

In this table and the following these the Bremsstrahlung doses were calculated for a 0.3 radiation-length thickness Tantalum target. The current density of the cathode was calculated using the measured k_n and measured I_n values for the given power of magnetrons.

Table 5 represents computed characteristics of a hypothetical X-band compact microtron that could be used as a 6 MeV gamma source. In this example, type-I injection and larger Ω are assumed, which results in a smaller number of orbits at the same energy and a higher capture efficiency (k_n) than was attained in the previously built microtrons. Note that the diameter of the final orbit and the magnet pole diameter at 6.5 MeV is also less than that of the 5.8 MeV microtron.

Table 5: Computed characteristics of a 6.5 MeV X-band compact microtron with the type-I injection

U_n, MeV	n	D_n, m	D_{Pole}, m	$I_{n,}$ mA	Ω	k_n, %	P_{RF}, MW	i_C, A/cm^2	Cathode	t_{Cath}, h	Dose power, R/min·m
6.5	15	0.164	0.196	8.8	0.8	3–4	0.375	44.9-51.3	Ta	<10	133

Type-I injection regime with m=2 is a few times more efficient than the Type-II with m=3 that was used in references [8] and [9], but that requires a higher power magnetron that is now available, but which was not available for the two earlier microtrons. However, the problem of the required high cathode current density described above will still exist in any X-band microtron design because small enough LaB_6 cathodes are not yet available. An additional problem is the large accelerating field, E_0, in the small sized RF cavity. In the case of the X-band microtron, we estimate the needed field to be E_0 = 82 MV/m, a very high value. High technology fabrication techniques and high precision manufacturing would be needed, which greatly increases the cost of the cavity, especially since the accelerator has to work reliably for the users.

b) C-band and S-band microtron parameters and comparison with X-band microtron parameters

The longer wavelengths of C-band and S-band compact microtron designs ameliorate the severe problems caused by the small cathode size and high field in the RF cavity. LaB_6 emitters provide higher current

density at lower temperatures than metallic cathodes, which greatly increases the lifetime of the cathode. Larger sizes of the RF cavity reduce requirements for very high technology and consequently cost of the accelerator. Table 6 shows a comparison of the (mainly RF cavity) operating parameters for three microtrons: a X-band (9.3 GHz), 6.5 MeV microtron, a C-band (5.85 GHz), 6.5 MeV microtron, and an S-band (2.8 GHz) 9.5 MeV microtron. The S-band energy was chosen to be 9.5 MeV to be consistent with our proposed prototype. The electric field in the X-band cavity is more than twice as high as that of the S-band cavity, and the beam power in the S-band case is over 10 times greater than the X-band case. The C-band parameters are also much more favorable than those of the X-band case.

Table 6: Operating parameters of accelerating cavity for X-band, C-band, and S-band RF frequencies

f, GHz	U_0, MeV	Ω	E_0, MV/m	P_{RF}, MW	P_r, MW	Q_0	β	P_{Beam}, kW
9.3	6.5	0.8	82.0	0.375	0.192	6000	1.55	53
5.85	6.5	1.0	64.5	1.0	0.281	6990	2.83	257
2.8	9.5	1.8	40.7	2.0	0.413	12350	3.85	588

Here: Q_0, β, P_{Beam} are Q-factor of the unloaded accelerating cavity, coupling coefficient of the cavity and pulsed power of the accelerated beam, respectively

The computed characteristics of the C-band compact microtron with the type-I injection are shown in Table 7.

Table 7: Computed parameters of the C-band compact microtron with type-I injection

U_n, MeV	n	D_n, m	D_{Pole}, m	I_n, mA	Ω	k_n,%	P_{RF}, MW	i_C, A/cm^2	Cathode	t_{Cath}, h	Dose power, R/min·m
6.5	12	0.212	0.263	37	1.0	3–4	1.0	47.0	LaB_6	<1000	643

The above parameters of the above C-band microtron look feasible if a single crystal LaB_6 cathode with the cross section 1.5 x 1.5 mm can be used. Such a cathode is not currently available, but could be developed by an R&D program. The required field value is calculated to be E_0 =64.5 MV/m, which may be feasible for reliable operation of the accelerating cavity.

A compact S-band microtron can deliver additional output capabilities if the energy is increased up to 9-10 MeV. Table 8 shows the computed characteristics and parameters for an S-band compact 9.5 MeV microtron with type-II internal injection and a 2.5 x 2.5 mm^2 cathode emitter.

Table 8: Computed characteristics of an S-band compact microtron with type-II injection

U_n, MeV	n	D_n, m	D_{Pole}, m	I_n, mA	Ω	k_n, %	P_{RF}, MW	i_C, A/cm^2	Cathode	t_{Cath}, h	Dose power, R/min·m
9.5	10	0.375	0.482	65	1.8	4–5	2.0	28.4	LaB_6	>1000	1778

Note that the estimated E_0 for the S-band accelerating cavity is about 41 MV/m, which will operate with greater reliability for users.

9.5 MeV electrons produce higher energy bremsstrahlung gammas than 6.5 MeV electrons. . Utilization of U-Be target at 9.5 MeV beam, [3], provides high the neutron production rate. For the S-band microtron shown in Table 8, we estimate that the neutron flux is up to $7 \cdot 10^{10}$ n/s. The neutrons can be used for diagnostics of explosive materials, fission materials and other applications. Extraction of the electron beam at various energies is also available in this microtron.

These comparisons show that the S-band microtron with a type-II injection scheme provides higher beam power, increased gamma production, longer cathode lifetime, and requires fewer orbit turns than the C-

band and X-band microtrons. Furthermore, the 9.5 MeV S-band microtron can produce significant neutron production rates by using an appropriate target.

V. Anticipated Public Benefits

Microtrons have been proven to be rugged, dependable, versatile, compact electron accelerators that can produce higher gamma ray doses than betatrons and comparable or higher does rates at lower cost than linacs. The prototype microtron that we are proposing is based on a novel combination of parameters: 9.5 MeV electron energy, S-wave frequency band, and Type-II injection, which can not only produce intense gamma-ray beams, but which can be simply be configured to produce high neutron fluxes. The electron beam can be extracted from the microtron at various energies to strike a gamma-ray production target or a neutron production target, or the electron beam can be used directly as a radiation source.

Commercial microtrons with the parameters of the prototype could be used as a source of gamma rays or neutrons in scanning systems for homeland security purposes to detect nuclear materials, explosives, or other contraband materials. The capability of producing high gamma ray or neutron doses would permit scanning of cargo containers moving faster than is currently possible, for example scanning of containers on fast moving freight trains or reducing traffic delays when scanning trucks.

In the commercialization phase, we envision producing a line of microtron models that are attractive for homeland security and/or other commercial applications. Examples of other models include the following:

- Smaller, more compact, lower energy microtrons, e.g. maximum energy 6.5 MeV or lower.
- More portable microtrons using permanent magnets instead of electromagnets and which operate on battery power could be used in environments in which electrical power and associated cables are not available.

Potential applications for these are: scanning baggage or freight in airline terminals, in-field scanning for faults in bridge structures and oil pipelines.

The extracted electron beam has a very precise energy, and a small beam size and divergence, which makes it especially useful for medical therapy or imaging applications.

In the commercialization phase we envision partnering with a manufacturer that has facilities to produce appropriate quantities of microtron systems of the model types described above. See the attached commercialization plan. Phase II is intended to transition from an R&D project to a manufactured product.

VI. Degree to which Phase I has Demonstrated Technical Feasibility

The purpose of the Phase I study was to study the technical feasibility of our original conceptual design of a portable, battery-operated microtron that could produce gammas with energies up to 6 MeV. Because microtrons operate with a fixed magnetic field, the magnet could be a permanent magnet that required no external power source. The smallest possible 6.5 MeV microtron that could produce gammas up to 6 MeV required use of X-band RF frequency.

The Phase I study expanded the choice of RF frequencies to include C-band and S-band frequencies and we considered additional important criteria such as engineering complexity and cost, manufacturing cost, gamma yield and ratio of yield to cost, availability of commercial components, expected lifetimes of

critical components. We evaluated the overall size and mass of the system: the radiation head, for which the mass is mainly that of the magnet, and the power components, such as the magnetron and modulator, and the necessary shielding mass. In addition, we studied three possible prototype magnet types, the original fully permanent magnet design, a hybrid design that supplemented the permanent magnet with electrical correction coils, and an electromagnet.

The phase I study focused not only on the eventual commercial version, but also on a prototype system that could be designed and built in Phase II. The addition of a control system suitable for prototype operation was also studied. The detailed results of the Phase I study are contained in this document. We believe we have met and exceeded the objectives of Phase I. The following conclusions were reached as a result of the Phase I studies:

- A relatively low-mass portable, battery-operated 6.5 MeV X-band microtron is technically feasible, but it has the following serious disadvantages and risks:
    - The small sizes of the X-band electron source and the RF cavity require high precision mechanical specifications, which lead to high fabrication costs. The small size of the cathode leads to short lifetimes (~10 hours), and requires frequent cathode replacements and high maintenance costs.
    - A purely permanent microtron magnet is technically feasible, but it would be more complicated to build. Built-in tuning blocks are needed to make corrections for field non-uniformity, and temperature compensators must be designed and integrated into the structure of the permanent magnet elements. A permanent magnet requires a mechanical/hydraulic fixture assembly and disassembly of the magnet due to the magnetic force between the halves. These could be implemented in commercial versions.
    - Battery operation has some advantages for portability and operating the system in the field, and development of more energy-efficient batteries is progressing, but it is not necessary to be implemented in a Phase II prototype system.
- The prototype system that we recommend to be built in Phase II has the following characteristics:
    - The S-band frequency range has more modest mechanical tolerances and lower fabrication costs. The expected cathode lifetime (~1000 hours) is much larger and more suitable for commercial operation. S-band is clearly the best choice for a prototype system.
    - The simplest, least costly and most practical magnet is an electromagnet, especially for a prototype. The field strength can be varied for over a large range, and it can be opened for changing components for testing and evaluation.
    - Instead of battery operation, the prototype system should be run off the normal electrical power or portable generators.
- The maximum microtron energy for the Phase II prototype should be raised from 6.5 MeV to 9.5 MeV. This will result in the following advantages:
    - The electron beam can be extracted or targeted at 6.5 MeV, which enables testing the gamma yields or doses at the same energies that were in the original topic description.
    - Accelerating the electron beam to 9.5 MeV provides a means to produce high neutron fluxes, which can be used to detect nuclear materials and explosives by neutron interactions in addition to gamma interactions. This added capability should be useful to homeland security applications as well as additional commercial applications.
    - Following Phase II, a series of microtrons can be produced, based on customer needs. For example, a smaller 6.5 MeV microtron can produce gammas by using production targets optimized for gamma production. Smaller, lower energy microtrons could be in the product line, as well as 9.5 MeV microtrons.

VII. References

[1] V. I. Veksler, DAN SSSR 43, 346 (1944); J. Phys. U.S.S.R. 9, 153 (1945).
[2] A.P. Grinberg, Usp. Fiz. Nauk 75, 421-458, 1961; Sov. Phys. Uspekhi, V 4, No 6, 857-879, 1962.
[3] S.P. Kapitza and V.N. Melekhin, The microtron, Harwood Academic Publishers, London, Chur, ISBN 0-906346-01-0.
[4] G. M. Kazakevich, V. M. Pavlov, G. I. Kuznetsov, Y. U. Jeong, S. H. Park, and B. C. Lee, J. Appl. Phys. 102, 034507 (2007).
[5] G.M. Kazakevich, V.M. Pavlov, Y.U. Jeong, B.C. Lee, PRST-AB 12, 040701 (2009)
[6] G. M. Kazakevitch, Y. U. Jeong, B. C. Lee, S. O. Cho, J. Lee, V. P. Belov, N. G. Gavrilov, "Magnetron Driven Classical Microtron as an Injector for a Wide Band Far Infrared Free Electron Laser" Proceed. of PAC01, 2739-2741, 2001.
[7] G. M. Kazakevitch, Y. U. Jeong, B. C. Lee, N. G. Gavrilov, M. N. Kondaurov, Nucl. Instr. and Meth. in Phys. Research, A 507 (2003) 146-149.
[8] V. Polyakov, F. Rodionov, B. Stepanchuk, Jour. Techn. Phys., 1971, *XLI*, 8, 1667-1671; Soviet Physics Technical Physics, V 16, No 8, 1311-1314, 1972.
[9] O. Brezhnev, G. Kazakevich, V. Ponomarchuk, E. Philippov, Instrun & Experiment. Techn., 1975, No 2, 17-19.
[10] R. J. Abrams, M.A.C. Cummings, R.P. Johnson, S.A. Kahn, G.M. Kazakevich, "Compact, Microtron-Based Gamma Source" Paper THPMR052, Proceedings of IPAC16, http://accelconf.web.cern.ch/AccelConf/ipac2016/papers/thpmr052.pdf
[11] S. Kahn, R.J. Abrams, M.A.C. Cummings, R.P. Johnson, G.M. Kazakevich "Magnet System for a Compact Microtron", Paper TUPMB026, Proceedings of IPAC16, http://accelconf.web.cern.ch/AccelConf/ipac2016/papers/tupmb026.pdf
[12] G.M. Kazakevich, R.J. Abrams, R.P. Johnson, S.A. Kahn and M.A.C. Cummings, "Microtron-based Intense Neutron Source", PaperTUPOY050, Proceedings of IPAC16, http://accelconf.web.cern.ch/AccelConf/ipac2016/papers/tupoy050.pdf

VIII. Addendum A: Feasibility of a battery-powered microtron

1. Power system requirements

The main elements requiring power are the magnetron and the electromagnet, unless a permanent magnet is used. A representative commercial magnetron that produces ~1 MW of pulsed power with a duty cycle of 0.001 requires ~2.5 kW of anode power including ~100W of heater power[1]. Other components such as electronics and vacuum pumps may require less than 1.5 kW of additional power, for an estimated total power of ~4 kW. Magnetron power supplies are available commercially. If an electromagnet is used, the power required for the coils is approximately 5 kW. Allowing a 1 kW margin, the total power required is 10 kW for estimation purposes

The battery energy capacity required depends directly on the length of time the system is operating on battery power and during the operation time, what percentage of the time the system is typically operating continuously. To provide 4kW of power by batteries for 10 hours of continuous operation would require 40 kWh of energy. By means of the energy density provided by current state of the art batteries, 400Wh/kg (see paragraph below) would therefore require a 100 kg battery pack. We envision the battery pack to be on a mobile cart, separate from the accelerator head, and connected by flexible power cables. If recharging the batteries must be done in a remote location in which there is no source of electric power, then the recharging could be done by a portable diesel generator or possibly by the engine of the vehicle that is used to transport the system to the site of operation. Depending on the required bremsstrahlung dose rate one can minimize the power consumption.

2. Available battery capacities

a. Some typical auto battery parameters

The development of high capacity rechargeable batteries has greatly advanced in recent years, mainly for supplying hybrid and electric vehicles.

- The 2015 Toyota Prius plug-in hybrid battery pack has a capacity of 4.4 kWh using a lithium ion battery set that weighs 176 lbs (80 kg), which indicates that the energy density is 55 Wh/kg.
- The battery set in the 2014 Tesla model S uses an array of 6000 Panasonic model 18360 lithium ion batteries to produce 60 kWh of energy, and are connected in groups wired in series to produce 300kW of power. The nominal capacity of the individual batteries is 2900 mAh at 3.6V, or 10.4Wh per 45.5 g battery, for an energy density of 229 Wh/kg. This figure does not take into account packaging or cooling liquid.
- In December, 2014, Seeo Corporation announced the introduction of a new "Drylite" lithium polymer battery, which does not require circulation of cooling liquid as required in the Tesla. Seeo claims that the Drylite batteries will provide an energy density of 400 Wh/kg.

b. Tesla Powerwall Units

In April of 2015Tesla launched its PowerWall series of wall-mountable batteries for home energy storage in conjunction with solar panels or for emergency backup power. The specifications[2] are listed below.

- **Technology** Wall-mounted, rechargeable lithium ion battery with liquid thermal control.
- **Model** 6.4 kWh, *$3,000* For daily cycle applications
- **Warranty** Ten years

[1] For example magnetrons available commercially from CPI include model SFD 313, an S-band 1 MW magnetron that is air cooled, and model VMS 1143B, a water cooled 3 MW C-band magnetron.

[2] Taken from the Tesla web site

- **Efficiency** 92.5% round-trip DC efficiency
- **Power** 3.3 kW
- **Depth of Discharge** 100%
- **Voltage** 350 – 450 volts
- **Current** 9.5 amperes

- **Compatibility** Single phase and three phase utility grid compatible.
- **Operating Temperature** -4°F to 122°F / -20°C to 50°C
- **Enclosure** Rated for indoor and outdoor installation.
- **Installation** Requires installation by a trained electrician. DC-AC inverter not included.
- **Weight** 214 lbs / 97 kg
- **Dimensions** 51.3" x 34" x 7.2"
  1302 mm x 862 mm x 183 mm
- **Certification** UL 9540, UL 1642, UL 1973
  AC156 seismic certification
  IEEE 693- 2005 seismic certification
  FCC Part 15 Class B

We note the following general characteristics:

- The energy density per unit is 640 Wh/kg, including packaging and liquid cooling, which is greater than the previously cited energy densities.
- The power produced is 3.3 kW. To supply the power needs of the microtron, 10 kW, would require 3 units, with a total weight of 300kg, approximately the mass of the microtron itself.
- Three units provide a total of 19.2 kWh of energy, enough to run the microtron for 19.2 hours between charges.
- No information was provided for the time needed for recharge the batteries
- The cost for 3 units is $9000, not including inverters and other electrical components such as transformers, and a powered mobile stand and installation.

For comparison, a typical 10 kW gasoline powered portable electric generator, priced at ~$3000 is shown below. In comparison with the Tesla PowerWall,

3. Gasoline-powered portable electric generator

The Briggs & Stratton model shown below is a typical 10 kW gasoline powered portable electric generator, priced at ~$3000.

Briggs & Stratton Professional 30556 - 10,000 Watt Electric Start Portable Generator

Weight:	295 Lbs. (133.81 kilograms)
Dimensions:	30"L x 27"W x 32"H (76.20 x 68.58 x 81.28 cm)

Product Specs

Voltage	120/240 Single-Phase
Frequency:	60 Hertz
Alternator:	Brush
Auto Voltage Regulation:	Yes
Fuel Type	Gasoline
Rated Amps:	42 Amps @ 240 Volts (Single Phase)
Portability Kit:	NeverFlat
Tank Size:	7 Gallons
Run Time (50% Load):	7 Hours
Fuel Tank Material:	Metal
Fuel Gauge:	Yes
Decibel Rating @ 7m:	Not Measured by Manufacturer
Idle Control:	Yes
Hour Meter:	Yes
Battery:	Included

4. Conclusions

Although the lithium batteries are steadily improving, they are not competitive with conventional portable electric generators at the present time. Tesla has at least entered the non-auto market with units that are packaged for use in homes or in the field. But for a 10 kW capability the battery pack weighs about three times as much as a comparable gasoline powered generator and costs at least 3 times as much. The operational time of the batteries for the microtron is about 1 day of steady operation – then recharging is needed or a spare battery set is needed, and recharging would require connection to the electrical grid or use of a portable electrical generator. The operational time of the electrical generator is limited only by the size of the fuel tank, and it could be outfitted with a larger fuel tank. Although battery power is a cleaner power source than gasoline, we conclude that battery power is not a practical option for the microtron at the present time or in the near future.

IX. Addendum B. Papers published in Proceedings of IPAC16

The following pages contain copies of the papers presented in references [10], [11], and [12] at the IPAC16 Conference.

THPMR052 Proceedings of IPAC2016, Busan, Korea

COMPACT, MICROTRON-BASED GAMMA SOURCE*

R. J. Abrams†, M. A.C. Cummings, R. P. Johnson, S. Kahn, G. M. Kazakevitch, Muons, Inc., Batavia, USA

Abstract

The conceptual design of a prototype S-band pulsed, 9.5 MeV compact microtron with type-II injection is described. Estimates of parameters such as beam current and cathode lifetime, and comparisons with X-band and C-band parameters are presented. The electron beam can be extracted at various energies up to 9.5MeV. Estimated yields of gammas produced at 6.5 MeV operation and estimated yields of gammas and neutrons produced at 9.5 MeV are presented.

INTRODUCTION

The microtron is a cyclic electron accelerator that operates on the Principle of Resonant Acceleration first proposed and developed by V. Veksler [1]. The "classic" microtron features a magnetic field that is constant and uniform over a circular region in which the electron trajectories are executed. Acceleration is provided by an RF cavity located at the point at which the electron trajectories pass as illustrated in Fig. 1.

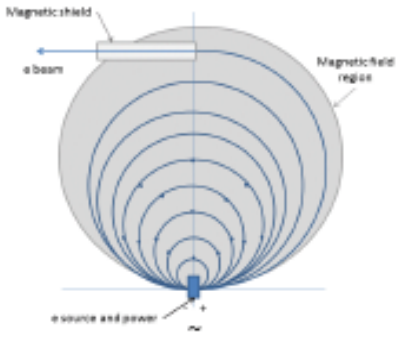

Figure 1: Simplified representation of a classic microtron. The source of electrons is a heated cathode within an injector. The acceleration is provided by a single RF cavity co-located with the source. Dots represent the RF periods in the first few orbits, e.g. the first orbit has 2 periods, the second has 3 periods, etc. Electrons can be extracted tangentially to the final orbit by means of a magnetically shielded tube, as shown. Alternatively, internal targets can be placed in the beam.

Electrons in the energy range from a few MeV up to ~ 10 MeV are used to produce gamma rays for a variety of applications, such as scanning for nuclear materials or explosives hidden in cargo containers or vehicles. By using appropriate targets photo-neutron reactions by the gammas produce useful fluxes of neutrons for active interrogation applications, particularly for electron energies near 10 MeV.

* Work supported by U.S. DOE SBIR grant DE-SC0013795

† email address boba247@muonsinc.com

MICROTRON PARAMETERS

A comprehensive exposition of the history and concepts of the microtron can be found in Ref. [2].

Basic Microtron Parameters

To satisfy the conditions of the principle of resonant acceleration, there are integer parameters, n and m, which are the number of orbits in the microtron and the number of periods that the accelerating field needs for the electron circulation along the first orbit. The parameter Ω, defined as H/H_C, where H is the magnetic field in the microtron, and H_C is the cyclotron magnetic field, in which period of revolution of electron with the total energy of m_0c^2 (its energy of rest) is equal to period of the accelerating field, $T_a=2\pi/\omega_a$.

For synchronicity, the fractional increase in electron total energy is

$$\Delta U/U = H/H_C = \Omega. \quad (1)$$

The integer parameter m, determines the length and dimension of the first orbit that completely encircles the cavity. The minimum value of m is 2, and two important relations involving n, and m, are the following.
The total energy of the n^{th} orbit electrons is:

$$U_n = (n+m-1)\,\Omega m_0c^2 \quad (2)$$

The diameter of the n^{th} orbit is:

$$D_n = (n+m-1)\,\lambda/\pi \quad (3)$$

λ is the wavelength of the accelerating field. These relations will be used in the following sections.

Design Alternatives

In addition to the basic microtron parameters above, there are design alternatives that are important for the performance of a microtron. One is the choice of the frequency band of the RF accelerating field.

Frequency band Eq. 3 shows that the frequency (and the corresponding wavelength) determines the diameter of the final orbit and that of the magnet. In addition the wavelength sets the scale of the Rf cavity and that of the injection source. Three wavelength bands are commonly used for compact microtrons: X-band (λ=3.2 cm), C-band (λ=5.1 cm), and S –band (λ=10.7 cm).

Injection type A second important design parameter is the injection type. Consider two injection types, type-I and type-II, as depicted in Figure 2 and Figure 3. Note that electrons emitted from the cathode which to not enter the proper trajectory to pass through the slit near the cathode are not shown; they are quickly removed by hitting a wall at low energy. In Type I injection, electrons emitted

ISBN 978-3-95450-147-2

from the cathode pass through one of the two larger slits before assuming the paths taken by the successive full orbits through the cavity. The value of Ω is $0.65 < \Omega < 1.7$.

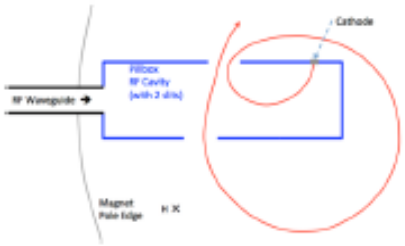

Figure 2: Initial trajectories of resonant electrons in a microtron using Type-I internal injection, based on [2].

In Type II injection, electrons emitted from the cathode, located near the symmetry axis of the flat-walled cylindrical cavity, pass through a small slit in the cavity wall, and make one revolution through the two larger slits before assuming the paths taken by the successive orbits through the cavity. The value of Ω is $1.7 < \Omega < 2.1$.

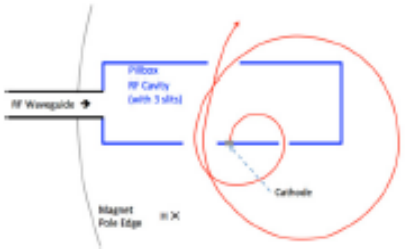

Figure 3: Initial trajectories of resonant electrons in a microtron using Type-II internal injection, based on [2].

The type-II injection scheme utilizes an additional radial slit in the median plane in the cavity cover for passage of the electrons along the first orbit. In type-II injection, Ω is greater, which allows a larger magnetic field, thus decreasing the diameter of the magnet and resulting in a more compact microtron. We have chosen type-II internal injection for the prototype.

Cathode heaters Compact microtrons have used various cathode designs with both direct and indirect heaters. Direct heaters have direct contact between the heating element, usually Ta, and the LaB_6 crystal, which causes diffusion of Ta into the LaB_6 and decreases the lifetime. Indirect heaters have a separation between the heating element and the LaB_6 crystal, such as shown in Figure 4, or heating by an electron beam, as shown in Figure 5. The final design may include a combination of the two types.

The injection parameters for S-band Type-II injection and C-band type-I injection are shown in Table 1, in which I_n/c_n is the ratio of current in the n^{th} orbit to the capture coefficient, D_C is the cathode diameter, E_0 is the electric field on the cavity axis, E_C is the electric field at the center of the cathode, i_C , is the current density at the cathode, and I_C is the cathode current. Note that $I_n/c_n < I_C$ for the S.band type-II case, which means that that the cathode temperature can be decreased, which further increases the cathode lifetime.

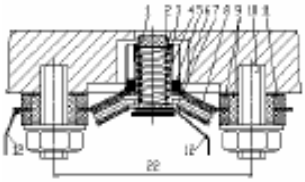

Figure 4: Layout of the microtron cathode assembly developed in Ref [3]: (1) emitter, (2) graphite holder, (3) cathode sleeve, (4) cylindrical filament, (5) heat shields, (6) carrying base, (7) tantalum plate, (8) ceramic insulators, (9) ceramic insulators, (10) titanium studs, (12) wire lead, reprinted from [3].

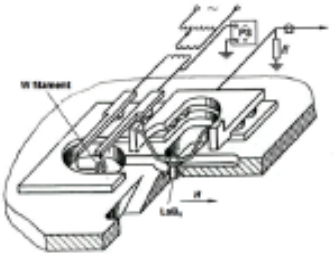

Figure 5: LaB6 cathode heated by an electron beam produced by a separate filament (reprinted from Ref. [2]).

Power system The RF system as depicted in Figure 6 is powered by a pulsed magnetron coupled to the accelerating cavity via a waveguide system that includes a ferrite insulator or a circulator with a matched load, a directional coupler and the waveguide vacuum window. The circulator and the matched load provide stable operation of the magnetron preventing discharges caused by a strong reflected wave. The magnitude of the reflected wave passing to the magnetron is reduced by 17-20 dB, which is enough for the reflected wave to stabilize the magnetron frequency. See [4], [5] for full discussion.

MAGNET AND BEAM EXTRACTION

The design of the magnet and the beam extraction system are presented in separate IPAC 16 contributions, references [6] and [7].

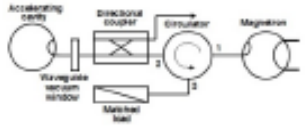

Figure 6: Schematic of the microtron RF system.

ISBN 978-3-95450-147-2

Table 1: Injection Parameters for C-band Type-I, 12-Orbit (n=12) and S-band Type-II, 10-Orbit (n=10) Microtrons

Microtron, injection	I_n/c_n (A)	Ω	D_C (mm)	E_0 (MV/m)	E_C (MV/m)	i_C (A/cm^2)	I_C (A)
C-band, type-I	1.057	1.0	1.5	64.5	21.7	43.5	0.69
S-band, type-II	1.778	1.8	2.5	40.7	32.4	55.6	2.23

Table 2: Comparison of 6.5 MeV X-, C-, and S-band Versions and 9.5 MeV S-band Compact Microtrons (Note that X-band and C-band Versions Use Type-I Injection and S-band Versions Use Type-II Injection)

U_n, MeV -Band	A (cm)	n	D_n (m)	D_{Pole} (m)	I_n (mA)	Ω	c_n (%)	P_{RF} (MW)	i_C (A/cm^2)	Cathode	t_{Cath} (h)	Gamma Dose (R/min·m)
6.5-X	3.2	15	0.164	0.196	8.8	0.8	3–4	0.375	44.9-51.3	Ta	<10	133
6.5-C	5.1	12	0.212	0.263	37	1.0	3–4	1.0	43.5	LaB_6	500	643
6.5-S	10.7	7	0.273	0.38	90	1.8	4–5	2.0	55.6	LaB_6	1000	860
9.5-S	10.7	10	0.375	0.482	65	1.8	4–5	2.0	28.4	LaB_6	>1000	1660

PERFORMANCE CALCULATIONS

Table 2 shows a comparison of the calculated characteristics for several versions of microtrons, including number of orbits (n), n^{th} orbit diameter (D_n), magnet pole diameter (D_{Pole}), currents, energy gain per turn, capture efficiency, RF power, cathode current density, cathode type and lifetime, and gamma dose. In addition to the values in the table, the estimated neutron yield at 9.5 meV is $7{\cdot}10^{10}$ n/s. An analysis of a higher intensity microtron-based neutron source is presented in another IPAC 16 paper [8].

SUMMARY

We have studied various microtron parameters for a high intensity gamma source and we summarize our findings.

Table 2 shows that although the 6.5 MeV X-band microtron is the most compact, it provides the lowest gamma dose, and an unacceptably short cathode lifetime. In addition, the small size of the accelerating structure precludes the use of a LaB_6 cathode, and requires high-precision machining and high costs. Further, S-band 6.5 MeV version produces 34% higher gamma done and has a 44% larger magnet diameter, offering a potential trade-off. The S-band 9.5 MeV S-band version produces more than 2-3 times greater gamma dose, with a magnet that is 30-40% larger than the S-band or C-brand versions. The 9.5 MeV also version can be operated at 6.5 MeV, or at other energies, and is our optimum design choice.

REFERENCES

[1] V. I. Veksler, DAN SSSR 43, 346 (1944); J. Phys. U.S.S.R. 9, 153 (1945).
[2] S.P. Kapitza and V.N. Melekhin, The microtron, Harwood Academic Publishers, London, Chur,ISBN 0-906346-01-0.
[3] G. M. Kazakevich, V. M. Pavlov, G. I. Kuznetsov, Y. U. Jeong, S. H. Park, and B. C. Lee, J. Appl. Phys. 102, 034507 (2007).
[4] G. Kazakevich, et al, PRSTAB 12, 040701 (2009).
[5] G. Kazakevich, et al, NIM A 647 (2011) 10-16.
[6] S. Kahn, et al, "Magnet System for a Compact Microtron," presented at IPAC'16, Busan, Korea, May 2016, paper TUPMB026.
[7] S. Kahn, et al, "Simulation of an Extraction System for a Compact Microtron," presented at IPAC'16, Busan, Korea, May 2016, paper TUPMB026.
[8] G. Kazakevich, et al, "Microtron-based Intense Neutron Source," presented at IPAC'16, Busan, Korea, May 2016, paper TUPOY050.

TUPMB026 Proceedings of IPAC2016, Busan, Korea

MAGNET SYSTEM FOR A COMPACT MICROTRON*

S.A. Kahn†, R.J. Abrams, M.A.C. Cummings, R.P. Johnson, G.M. Kazakevich, Muons, Inc., Batavia, IL, U.S.A.

Abstract

A compact microtron can be an effective gamma source that can be transported to locations outside the laboratory. As part of a Phase I study we have studied a portable microtron that can accelerate electrons with energies of 6 MeV and above as a source for gamma and neutron production. The mass of the magnet is a significant contribution to the overall mass of the system. This paper will discuss conceptual designs for both permanent magnet and electromagnet systems. The choice of microtron RF frequency range is determined by the application requirements. The RF frequency band influences the size of the microtron magnet and consequently its weight. We have looked at how the design would vary with the different frequency configurations.

INTRODUCTION

There is a growing need for compact accelerators for security and medical applications. These applications may involve the ability to transport the accelerator to outside locations where operating resources may be limited. A microtron can accelerate electrons to 6 MeV and above with intensities 10 to 100 times greater than with a betatron. The electron beam can be extracted to targets for gamma ray production. With a microtron designed to produce electrons with energies greater than 9 MeV, the microtron can with an external target be an intense neutron source. This paper describes the magnet system for a compact microtron. The dimensions of the magnet vary with the RF frequency. Higher frequency microtrons have smaller dimensions and consequently weigh less. The frequency choice does depend on the application. In this study we have looked at magnet designs for X-band, C-band and S-band microtrons. Table 1 summarizes the parameters used to describe a microtrons in each of these frequency bands. Similar parameters are shown for the 6.5 MeV and 9.5 MeV microtrons with the difference being the number of orbits before extraction.

Although the X-band microtron would be smaller and lighter which would be beneficial for portability the lifetime of the emitter cathode is too short to be practical and replacement of the emitter would require breaking the vacuum seal and opening the RF cavity making this less desirable.

Table 1: Microtron Parameters

Parameter	Unit	X-band	C-band	S-band
Frequency	GHz	9.3	5.85	2.8
Wavelength	mm	32	51	107.1
Cyclotron Field	Oe	3319	2088	1000
Magnet Field	Oe	2655	2506	1800
ΔE per turn	mc^2	0.8	1.2	1.8
6½ MeV Turns		15	12	7
9½ MeV Turns			15	10
Cathode Lifetime	hrs	10	500	1000

We have examined three candidate magnet designs. These included (1) a permanent magnet without coils, (2) a hybrid magnet where the dominant part of the field comes from the permanent magnet material, but with trim coils to provide some variation of the magnetic field for tuning and (3) a conventional magnet with copper coils and iron poles.

The uniformity of the magnet field is an important consideration. The field must be uniform over the region where the beam traverses with a field non-uniformity error $\Delta B/B<1/n^2$ where n is the number of orbital turns in the microtron.

PERMANENT MAGNET OPTION

The advantage of using a permanent magnet is that no power supply would be necessary. This could be very important for operation away from a location where electricity and cooling water may not be readily available. Permanent magnet materials that have been used for magnets include Alnico, ferrite, neodymium ($Nd_2Fe_{14}B$) and samarium cobalt ($SmCo_5$ and Sm_2Co_{17}). Although Alnico has a large remnant field (B_R), it has a strong demagnetization curve because of its small coercivity which makes it undesirable. Ferrites have been previously used for accelerator applications, but it does not have a large enough B_R. The cobalt in the SmCo material can become strongly radioactive from the beam and this material tends to be more expensive. Neodymium is the best choice for permanent magnets and it is used for many industrial applications. The large variation in B_R with temperature is a concern. This is particularly true for operation outside of a temperature controlled environment. A temperature compensation scheme would be necessary for using the permanent magnet option. This will be discussed.

Figure 1 shows an R-Z sketch of a template to define the geometry using a permanent magnet. The geometry parameters shown in the figure depend on the cavity frequency and the output beam energy. Table 2 shows the parameters found for the S-, C-, and X-band configurations.

* Work supported by U.S. D.O.E. SBIR grant DE-SC0013795
† email address: kahn@muonsinc.com

ISBN 978-3-95450-147-2

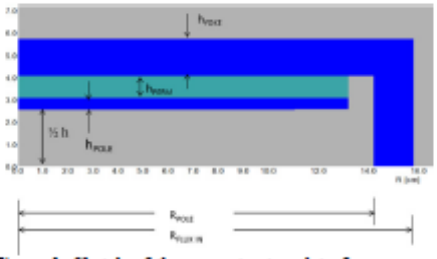

Figure 1: Sketch of the geometry template for a permanent magnet microtron. The figure defines the parameters.

Table 2: Geometry Parameters of a Permanent Magnet Microtron for Different Frequency Bands

Symbol	Description	X-band	C-band	S-band
H	Gap Height	32	51	107
N	Number of Turns	15	12	12
D_N	N-turn Diameter	196	212	443
R_{POLE}	Pole Radius	98	131	275
h_{POLE}	Height of Iron Pole	10	10	10
h_{Nd}	Height of Neo	10	10	15
h_{YOKE}	Height of Yoke Top	13	16	20
$R_{FLUX\ IN}$	Inner Radius Flux Rtn	108	141	285
$R_{FLUX\ OUT}$	Outer Radius Flux Rtn	121	156	310
W	Magnet Mass	24 Kg	46 Kg	247 Kg

There must be enough iron not only to achieve the maximum field from the permanent magnet, but also to minimize the stray fields outside the magnet. As we also want to minimize the weight of the magnet, the thickness of the flux return was chosen to keep the permeability greater than 100 (the minimum at a local spot at the end of the pole). The magnet mass for the different configurations considered is shown in Table 2.

An important issue for permanent magnet material is its dependence on temperature. For most magnetic materials the change in magnetization $\frac{d\log(B_R)}{dT}$ is approximately constant over a large temperature range. The rate of variation is largest for those materials close to their Curie temperature. There is a correlation between B_R and the temperature dependence parameter d $\log(B_R)$/dT where the neodymium material with larger B_R also has a larger temperature variation. We have chosen to use the material with the smaller temperature dependence which has B_R=1.1 T and d $\log(B_R)$/dT=–0.08%/°C. The approach to temperature compensation is to provide in addition to the permanent magnet material a magnetic shunt whose flux falls faster with temperature than the permanent magnet material. Ni-Fe and Ni-Cu alloys have been used as shunts for temperature compensation. Ni-Fe with 30% Ni appears to be an optimal choice. The ratio of the Ni-Fe shunt to $Nb_2Fe_{14}B$ material is 19%. $Nb_2Fe_{14}B$ is commercially available in a number of sizes. Figure 2 shows an array of 1"×1"×3/8" blocks with Ni-Fe strips between the blocks for temperature compensation.

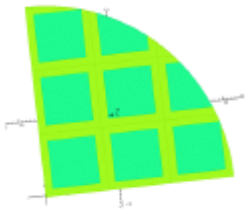

Figure 2: A quarter of the magnetic pole comprised of $Nb_2Fe_{14}B$ blocks arranged in an array with Ni-Fe strips interleaved for temperature compensation.

There are certain issues associated with using the neo-dymium material. Each block is attracted to the adjacent iron with a force of 30 to 55 lbs (depending on the B_R chosen). Disassembling the blocks from the pole steel would be very difficult. Specification sheets of the per-manent magnet material indicate that the material can have a ±3% variation of B_R. There is also a large varia-tion of the polarization direction. The variation can be reduced by rejecting samples with large deviations which can increase the cost. We have performed a study where the magnet was composed of material with a B_R variation of ±3%. The ΔB/B non-uniformity in the aperture was examined as a function of the iron pole thickness. With h_{POLE}=10 mm ΔB/B would be 0.2%. The permanent magnet would need a separate vacuum-sealed chamber, which would increase the complexity and weight of the microtron. Disassembly and reassembly of the permanent magnet microtron may introduce positioning errors of the vacuum chamber relative to the magnet. A permanent magnet precludes varying the field or changing the microtron energy. Because of the short lifetime of the cathode for the X-band microtron the use of a permanent magnet may not be feasible.

As an additional alternative we have examined using the permanent magnet option but adding trim coils to provide some ability to tune the magnetic field so that the beam will arrive at the cavity with the proper phase. Since the demagnetization curve for $Nb_2Fe_{17}B$ is linear over a large range, the magnetization will return to its original value when the current is turned off, one can add coils to the permanent magnet so long as the field from the coils does not exceed the linear range of the demagnetization curve. The current carried in the trim would be much smaller than that necessary to provide the entire field. The simu-lations showed that this would be a viable alternative, however to change the energy of the microtron in a notable range would need an electromagnet with significant current. The problems of disassembly of the hybrid magnet would be the same as the permanent magnets.

ISBN 978-3-95450-147-2

ELECTROMAGNET OPTION

Magnets with coils have been typically used for microtron applications. These magnets need ample power for their operation and could require cooling for the power generated in the coils. Using coils allows greater flexibility. The magnet field could be varied to allow tuning to keep the beam on resonance in the microtron. It could also be used change the output energy by varying the magnetic field.

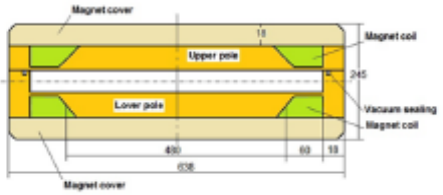

Figure 3: Template of electro-magnet geometry.

Figure 3 shows a sketch of an electro-magnet that was used as a template for the microtron magnet. In this figure the iron pole and flux return serve as the vacuum containment with an indium seal between the upper and lower poles. The coils have a trapezoidal shape to provide a better shaping of the field at larger radius. Table 3 shows the parameters for the electromagnet geometry for different microtron configurations. The design criteria were to minimize the magnet weight, to keep the iron permeability greater than 100 and to keep the current density to approximately 3 A/mm^2.

The table also shows the total mass of the magnet system for the different frequency bands for the Fig. 3 design. Much of the central part of the flux return top hat is not saturated and can be removed to reduce the magnet weight. The reduced mass is shown in the last line of the table. The mass of the electromagnet is significantly larger than the corresponding permanent magnet system. One can still imagine that microtron with the electromagnet could be put on a truck for mobility. The magnet pole can be shaped to provide the high field uniformity necessary for the microtron magnet. Figure 4 shows the field profile for the S-band magnet after the optimization of the pole shape. The figure shows that the largest deviation in field over the region where beam is present can be held to $\Delta B/B=0.00024$.

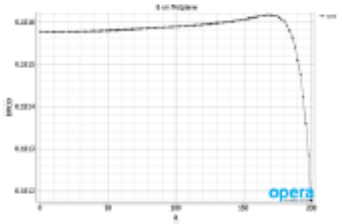

Figure 4: Optimization of the field profile for the S-band magnet.

CONCLUSIONS

We have investigated the design of a magnet for a transportable microtron to be used as a gamma and neutron source. We have examined the use of a permanent magnet system, but we favour a system where tuning would be possible. We have examined systems with different RF frequency ranges. The smaller and lighter X-band system was ruled out because the lifetime of the emitter system was too short to be commercially practical. The S-band system was chosen for our future R&D studies.

Table 3: Parameters Describing Electromagnet Geometry

Symbol	Parameter Description	Units	S-Band I	S-Band II	C-Band	X-Band
U	Final Beam Energy	MeV	6.5	9.5	6.5	6.5
H	Magnetic Field	T	0.12	0.18	0.2088	0.2655
R_{pole}	Mean Inner Coil Radius	mm	326	241	132	102
h_r	Flux Return Width	mm	28	26	18	18
h_y	Upper Yoke Height	mm	25	26	24	22.5
h_{pole}	Height of Pole and Coil	mm	35	59	35	29
R_{yoke}	Outer Yoke Radius	mm	408	326	201	170
I	Current in Each Coil	A turns	5513	9234	4585	3492
J	Current Density	A/mm^2	3	2.85	2.77	3
h_{coil}	Coil Height	mm	35	54	28	24
b_{coil}	Coil Width	mm	107.5	60	56	48.5
W	Total Magnet Mass	Kg	439	339	96	61

ISBN 978-3-95450-147-2

TUPOY050 Proceedings of IPAC2016, Busan, Korea

MICROTRON-BASED INTENSE NEUTRON SOURCE

G. Kazakevich#, R. Abrams, M.A.C. Cummings, R. Johnson, S. Kahn, Muons, Inc.,Batavia, IL, USA

Abstract

An L-Band, 7.7-9.8 MeV, CW, relatively inexpensive microtron with a warm accelerating cavity for multi-purpose applications in nuclear medicine and radiation industry is proposed. The microtron, with a photo-neutron converter, is intended to serve as an intense source of photo-neutrons with yield up to $4 \cdot 10^{12}$ n/s for nuclear medicine or/and production of short-lived isotopes, as a source of gamma-radiation with dose rates up to 130 kR/min·m with a heavy bremsstrahlung target, and as a source of electron beam with total energy of 9.8 MeV at an average current up to 4.4 mA for various radiation treatments.

INTRODUCTION

Relatively inexpensive and compact intense sources of electrons with energy up to 9-10 MeV at a beam power of a few tens of kW are interesting for application in medicine (as sources of intense photo-neutrons for boron-capture cancer therapy, production of short-lived isotopes, sterilization of medical waste, etc.) and industry (radiation treatment, sterilization, etc.). The classical warm-cavity microtron operated in CW mode may well solve the listed problems. In the literature, [1, 2], were proposed and considered such L-band projects, however they were not realized yet generally, we assume, because of absence of inexpensive, CW high power RF sources. Now industry produces L-Band magnetron RF sources with a power cost of $1.00 per Watt, thus the microtron projects represent an interest for customers. We propose and consider a design-project of such an L-Band, CW, laboratory-size classical microtron with total energy of 9.8 MeV as an intense source of γ-rays and photo-neutrons for various applications in medicine and industry. The total energy of the extracted beam can be varied in the range of 7.7-9.8 MeV. The microtron can operate in CW or pulsed mode with repetition rates up to 100 kHz and high duty-factor. It does not require the cryogenic equipment. The microtron is assumed to be easily controlled, reliable and stable in operation. Parameters of the CW microtron and its subsystems are presented and discussed here.

DESIGN PARAMETERS OF THE CW MICROTRON

One considers the type-I injection scheme microtron with the resonant frequency, f, of 1.5 GHz. The cyclotron magnetic field at this frequency, H_C, is ≈ 535 Oe. The magnetron RF source power, P_{ig}, is assumed to be 200 kW. This power presently is available with commercial generators. The total energy of the accelerated beam at the number of orbits, n = 23 is $U_n \approx 9.8$ MeV. This avoids photo-neutron activation of the microtron components. Using the type-I injection scheme with the microtron magnetic field, $H = \Omega \cdot H_C$, where Ω = 0.8, one can provide laboratory-scale sizes of the microtron magnet with diameter of the n-th orbit of $D_n \approx 1.73$ m, at the accelerated beam power, P_e, of 30-40 kW, Table 1.

Table 1: Design Parameters of the 1.5 GHz CW Microtron

n	U_n, MeV	P_{ig}, kW	D_n, m	m_{Mag}, kg	P_e, kW
23	9.81	200	1.727	$\approx 2.8 \cdot 10^3$	40.9

Note that the required inhomogeneity of the magnetic field for n = 23, $\Delta H/H \leq n^{-2} \approx 1.9 \cdot 10^{-3}$, is technically feasible.

RF SYSTEM OF THE CW MICROTRON

The RF system of the CW microtron represents a respective magnetron generator coupled with a pillbox-type accelerating cavity, Fig. 1, via a ferrite circulator and directional couplers for measurements of the generator and the acceleration parameters. Vacuum in the accelerating cavity is separated from dry nitrogen at atmospheric pressure in the waveguide system by a vacuum waveguide window.

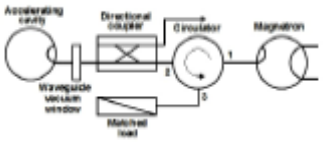

Figure 1: Conceptual scheme of the microtron RF system

The scheme provides stable operation of the microtron. At a circulator inverse loss of 17-20 dB the magnitude of the reflected wave passing towards the magnetron is enough to stabilize the magnetron frequency, making the generation frequency-locked by the reflected wave, [3, 4].

Assuming RF losses of the RF system, P_S, ≈1 dB on can estimate RF power, P_{Acc}, allowable for acceleration:

$$P_{Acc} = P_{ig} - P_S - P_{wl}.$$

Here P_{wl} is power lost in the walls of the RF cavity, [2]:

$P_{wl} \approx \frac{1.02\sigma}{\lambda}\left(1.2 + \arcsin\frac{1}{1.88s}\right)s^2\Omega^2 P_0$, where σ is conductivity of the cavity walls, $\lambda = c/f$, $s = E_\theta/H$, E_θ is strength of the RF electric field on the cavity axis, and P_0=8700 MW is the characteristic electron power. In microtrons about half of RF power is lost for acceleration of non-resonant electrons. Thus the coupling coefficient of the RF cavity with a waveguide, β, is: $\beta = P_{Acc}/(0.5 \cdot P_{wl}) + 1$. This allows a determination of

#grigory@muonsinc.com

ISBN 978-3-95450-147-2 08 Applications of Accelerators
2014 U04 Security

the loaded cavity Q-factor: $Q_L=Q_0/(\beta+1)$; Q_0 is determined by the cavity geometry. Parameters of the RF system for the injection scheme with β=0.94, [2], are shown in Table 2. The parameters correspond to a beam power of ≈40 kW.

Table 2: RF Parameters of the CW Microtron

λ, m	P_0, kW	P_{wl}, kW	P_{Acc}, kW	β	Q_L
0.2	41	77.1	81.8	2.06	$4.88\cdot10^3$

In accordance with data Tab. II the RF and beam power lost in the cavity is 118 kW with a cavity surface of 550.5 cm2. This corresponds to a power density of ≈214.4 W/cm2. Such a heat sink with good cooling looks feasible.

Since 100 kW CW magnetron generators with a cost per unit power of ≤$1 are consistent with current manufacturer capabilities, one can consider a widely tunable (in power) CW, two-channel magnetron generator, Fig. 2, based on magnetrons with power combining, [5]. The power control is provided by the controlled phase shift of signals driving both channels. Such a generator allows operation of the microtron in CW and pulsed modes. In the latter case the minimum pulse duration can be a few μs at a repetition rate of hundreds kHz. One can expect that the cost of power in such a generator also should be ~$1 per Watt.

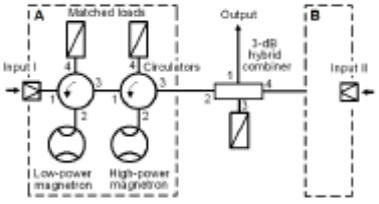

Figure 2: Conceptual scheme of the two-channel power-controlled magnetron RF source with power combining.

INJECTION IN THE CW MICROTRON

In accordance with the type-I injection scheme, [2], simulations of the injection were performed, Fig. 3.

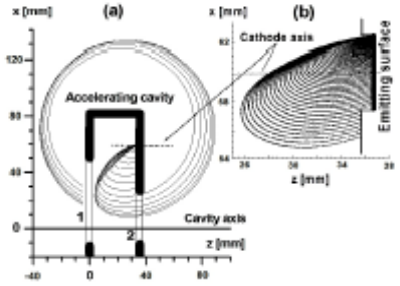

Figure 3: (a) 2-D tracking of the first orbit. With numbers 1 and 2 are marked the narrow slits directed along the x axis and used for input-output of the electrons. (b) 2-D tracking of the back-streaming electrons hitting the emitter.

In the simulation, the LaB_6 cathode emitting surface was recessed in a hole below the internal surface of the pillbox. The hole for the recessed emitter acts like a lens and provides some focusing of the injected electrons. For a hole of radius r_H and a recession depth d_C the RF field in the cathode surface center is, [6]:

$$E_{CS} \cong E_0 \cdot J_0(k_0 \cdot R_C) \cdot \cos(\varphi_s) \cdot \frac{J_0(k_r, r)}{\cosh(k_z \cdot d_C)} \approx 7.2 \text{ MV/m}$$

Here J_0 is the Bessel function of the first kind,

$E_0 = \frac{\Omega m_0 c^2 \cdot (\theta/2)}{e \cdot l \cdot \sin(\theta/2) \cdot \cos\varphi_s}$ is the maximum field on the cavity axis, l is the cavity length, $k_r = \chi_{01} / r_H$, where $\chi_{01} = 2.405$ is the first zero of the Bessel function and $k_z = \sqrt{k_r^2 - k_0^2}$, φ_s is the equilibrium phase for the microtron.

Considering the Schottky effect one can express the current density of a LaB_6 single crystal emitter as a function of (r, φ) as:

$$i_C(T, r, \varphi) = AT^2 \cdot \exp\left[\frac{-e\phi_C + 3.79\cdot10^{-4}\cdot\sqrt{E_{CS}(r,\varphi)\cdot10^6}}{k\cdot T}\right].$$

Here: A=73 A/K^{2}cm^2 and $e\phi_C$ = 2.66 eV are the Richardson constant and the work function for LaB_6, respectively, k is the Boltzmann constant and T is the emitter temperature in Kelvin. The initial value of the emission current at the emitter radius r_C is equal to, [6]:

$$I_C(T) = \int_0^{2\pi}\int_0^{r_C} i_C(T, r, \varphi) \cdot r \, dr \, d\varphi .$$

From the simulations, it follows that at the cathode temperature of 1650 K the current emitted by 5 mm-diameter single-crystal LaB_6 emitter will exceed 200 mA. It is enough to provide a beam power of 40 kW. The quite low temperature of the cathode will increase the cathode life time to a few thousands hours. Design of the indirectly heated cathode with the LAB_6 emitter is shown in Fig. 4, [6].

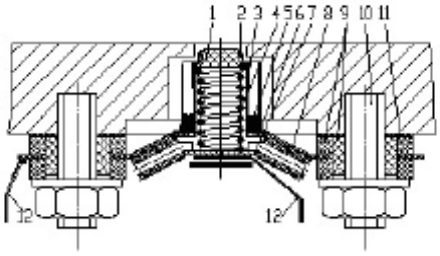

Figure 4: Layout of the microtron cathode assembly. 1- emitter, 2- graphite holder, 3- cathode sleeve, 4- cylindrical filament , 5- heat shields, 6- carrying base, 7-

ISBN 978-3-95450-147-2

tantalum plate, 8, 9- ceramic insulators, 10- titanium studs, 11- spacer, 12- heater contact.

The 5 mm-diameter [100]-face LaB_6 single crystal tablet-shape emitter is fixed in the graphite holder. The emitter thickness is 1.1 mm. The graphite holder prevents the diffusion of boron inside tantalum components of the assembly; that significantly increases the cathode life time. The cathode is mounted on two titanium studs screwed into the cavity cover, so that the cathode assembly is recessed in the cavity cover. The depth to which the emitting surface is recessed into the cover can be adjusted with the spacers.

MAGNETIC-VACUUM SYSTEM OF THE CW MICROTRON

The combined magnetic-vacuum system of the CW microtron is assumed to be sealed by an indium wire between the upper and lower poles of the magnet, [7]. A schematic of the generic microtron magnet is shown in Fig. 5.

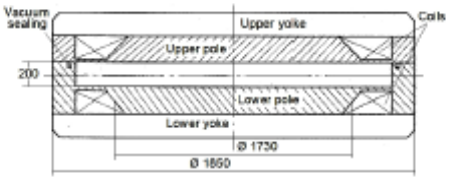

Figure 5: Sketch of the 9.5 MeV tubeless generic microtron magnetic-vacuum system. All sizes are in mm.

Since main parts of the magnet yoke are far from saturation, performed simulations show achievable inhomogeneity of the magnetic field of ~ $3 \cdot 10^{-5}$ for all orbits. This value is much less than the n^{-2} requirement. It allows optimization of the yoke sizes reducing the microtron weight.

The electron beam will be extracted by installing a magnetic channel of soft steel inside the microtron magnet at a tangent to the circular trajectory at the final orbit such the beam exits along the tangent. The extraction system allows compensation of perturbation of the magnetic field in the neighborhoods of the previous orbits resulting from the magnetic channel, by choosing the geometry of the magnetic rods, Fig. 6. The system was tested in a pulsed S-band microtron, [8], demonstrating 90-95% efficiency in extraction of the beam from the 4 last orbits. The extraction system will be simulated to reach highest extraction efficiency by compensation of perturbations of the magnetic field.

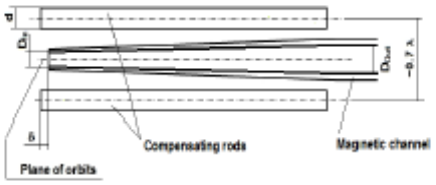

Figure 6: The extracting system of the L-band microtron.

GAMMA AND NEUTRON YIELDS OF THE CW MICROTRON

The bremsstrahlung dose power of the microtron at a distance of 1 m from a tungsten 0.3 radiation length-thick target, estimated in accordance with [2] is ≈130 kR/min.

The photo-neutron yield from U-Be target at a microtron beam power of 40 kW is estimated as $4.1 \cdot 10^{12}$ n/s, [2], at the optimal thickness of the target. Note that the beam power requires a dual-circuit cooling of the photo-neutron target. The expected bremsstrahlung dose powers and the photo-neutrons yields vs. the beam total energy at the accelerated beam power of $W_{kin}/2 \approx 41$ kW are shown in Table 3.

Table 3: Radiation Parameters of the CW Microtron

n	U_n, MeV	Dose, R/min·m	Neutrons yield, n/s
19	7.7	$80 \cdot 10^3$	$2.3 \cdot 10^{12}$
21	8.5	$115 \cdot 10^3$	$2.9 \cdot 10^{12}$
23	9.8	$128 \cdot 10^3$	$4.1 \cdot 10^{12}$

Note that U_n<8 MeV allows avoiding of photo-neutrons from the tungsten target.

REFERENCES

[1] S.P. Kapitza, The CW Microtron, in Coll. Pap. "High Power Electronics", V 4, 1965, pp. 165, (In Russian).
[2] S.P. Kapitza and V.N. Melekhin, in "The Microtron", Harwood Academic Publishers, London, Chur, 1978.
[3] G.M. Kazakevich, V.M. Pavlov, Y.U. Jeong, B.C. Lee, PRST-AB 12, 040701 (2009).
[4] G.M. Kazakevich, V.M. Pavlov, Y.U. Jeong, and B.C. Lee, NIM A 647 (2011) 10-16.
[5] G. Kazakevich, R. Johnson, B. Chase, R. Pasquinelli, V. Yakovlev, "Regime of a wideband phase-amplitude modulation in a CW magnetron transmitter with a phase control", http://arxiv.org/abs/1407.0304
[6] G. M. Kazakevich, V. M. Pavlov, G. I. Kuznetsov, Y. U. Jeong, S. H. Park, and B. C. Lee, J. Appl. Phys. 102, 034507 (2007).
[7] G. M. Kazakevitch, Y. U. Jeong, B. C. Lee, S. O. Cho, J. Lee, V. P. Belov, N. G. Gavrilov, "Magnetron Driven Classical Microtron as an Injector for a Wide Band Far Infrared Free Electron Laser" in Proc. PAC01, Chicago, USA, 2001, paper WPPH115, pp. 2739-2741.
[8] G. M. Kazakevitch, Y. U. Jeong, B. C. Lee, N. G. Gavrilov, M. N. Kondaurov, NIM, A 507 (2003) 146-149.

ISBN 978-3-95450-147-2